Emil Gorm Dahlbæk Nielsen, Niels Bohr Institutet

Speed of sound and higher-order $[p_{\mathrm{T}}]$ fluctuations in Pb–Pb collisions at $\sqrt{s_{\mathrm{NN}}} = 5.02$ TeV

- on behalf of the ALICE Collaboration

emil.gorm.nielsen@cern.ch

SQM2024

The 21st International Conference on Strangeness in Quark Matter
3-7 June 2024, Strasbourg, France

QGP in ultra-central collisions

Ultra-central collisions: fixed volume V

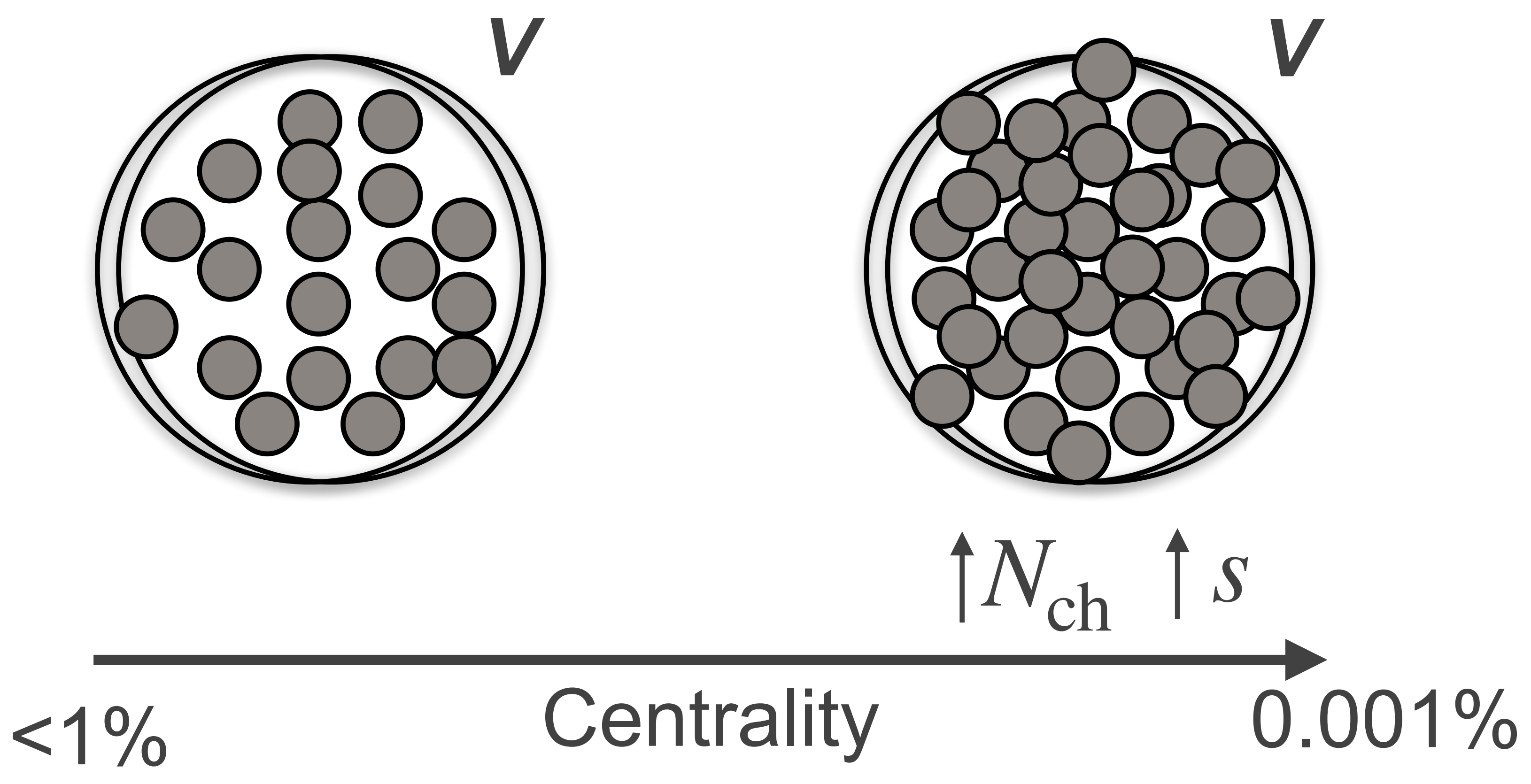

[L. Van Howe, PLB 118 (1982) 138]

Thermalised system: $\uparrow s \Rightarrow \uparrow T \Rightarrow \uparrow \langle p_{\rm T} \rangle$

$$\langle p_{\rm T} \rangle \sim 3T_{\rm eff}$$

[F. Gordium et al., Nature Physics 16, 615-619 (2020)]

Speed of sound, c_s^2, from thermodynamic relations

$$c_s^2 = \left.\frac{sdT}{Tds}\right|_{T_{\rm eff}} = \frac{d\ln\langle p_{\rm T}\rangle}{d\ln(N_{\rm ch}/d\eta)}$$

[F. Gardim et al., PLB 809 (2020) 135749]

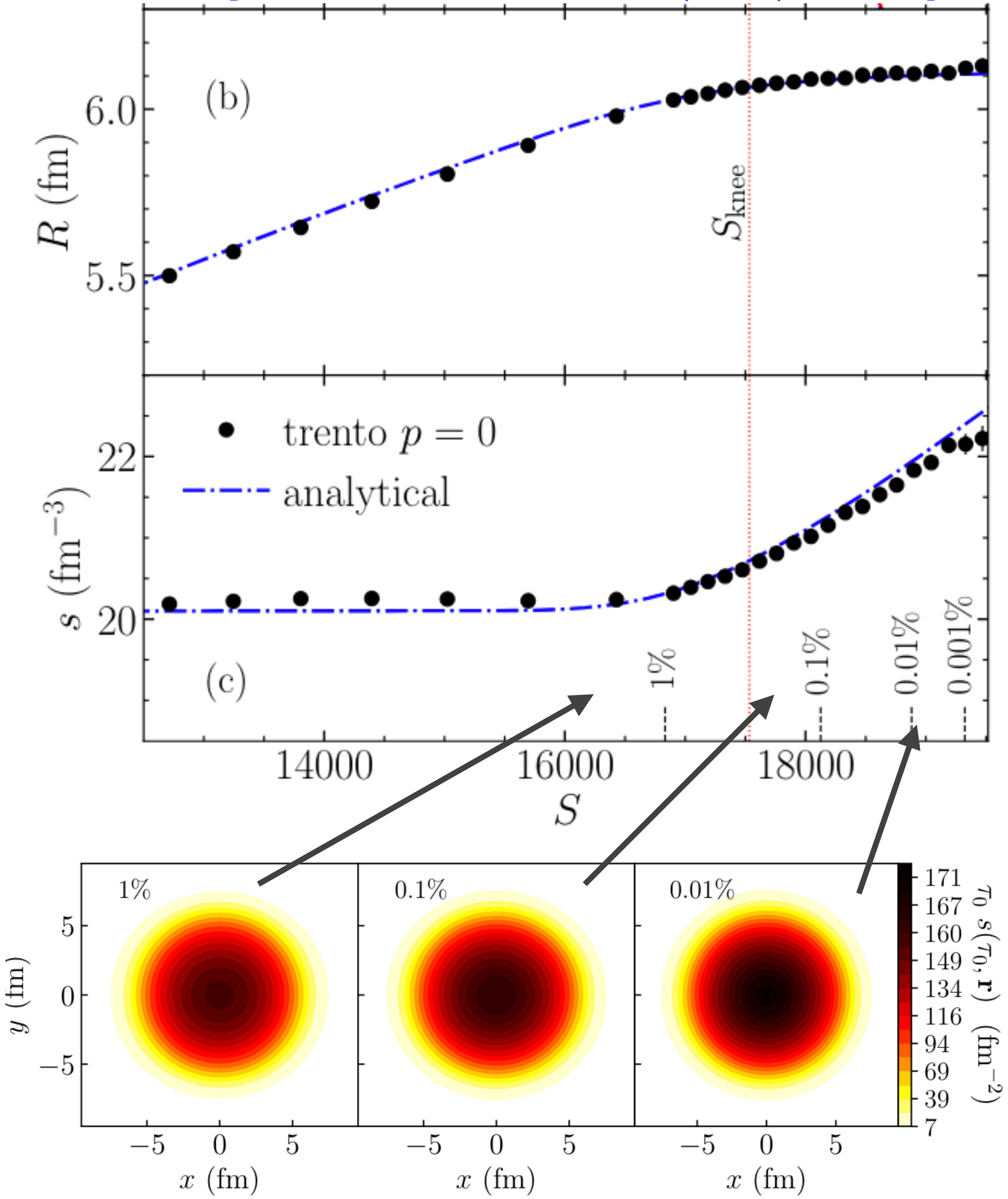

What determines the slope?

Recent theoretical studies suggest that the extraction of the speed of sound is heavily dependent on the centrality determination and associated η range.

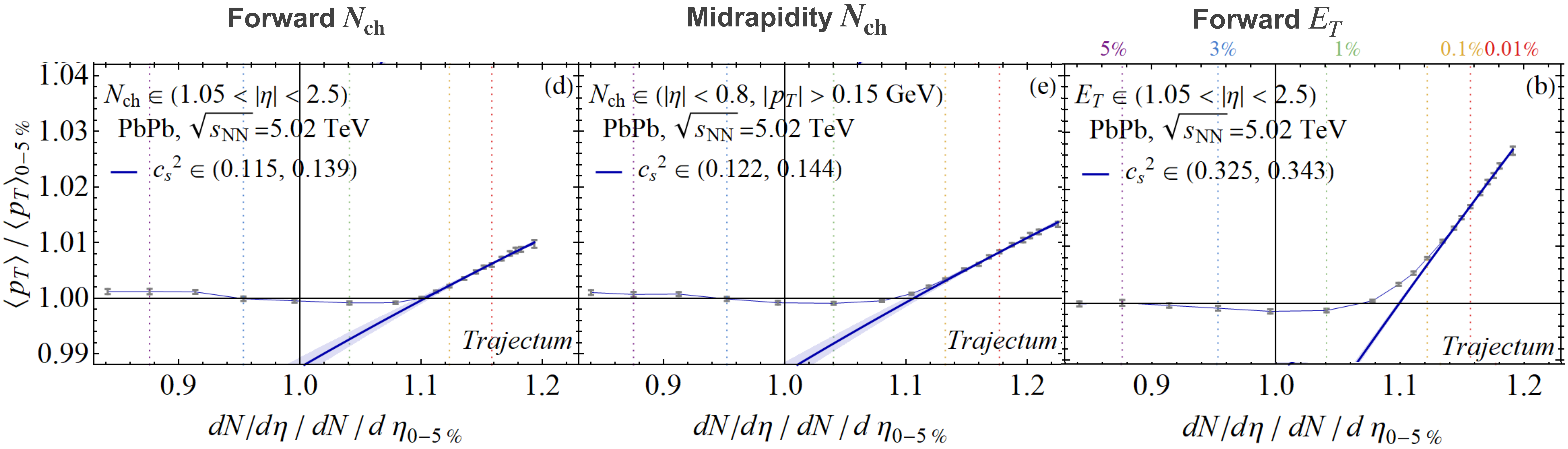

[G. Nijs & W. van der Schee, PLB 853 (2024) 138636]

Transverse momentum fluctuations

The fluctuations of the event-by-event mean transverse momentum, $[p_{\mathrm{T}}]$, arise from two sources:

[R. Samanta et al., PRC 108 (2023) 024908]
[R. Samanta et al., PRC 109 (2024) L051902]

Geometrical fluctuations

- Radial flow: hydrodynamic response of $[p_{\mathrm{T}}]$ to the inverse size $1/R$
- At fixed multiplicity → radial flow fluctuations from fluctuations of inverse size

Intrinsic fluctuations

At fixed impact parameter *b*

- Quantum fluctuations in wave function of incoming nuclei
- Thermal fluctuations of the QGP

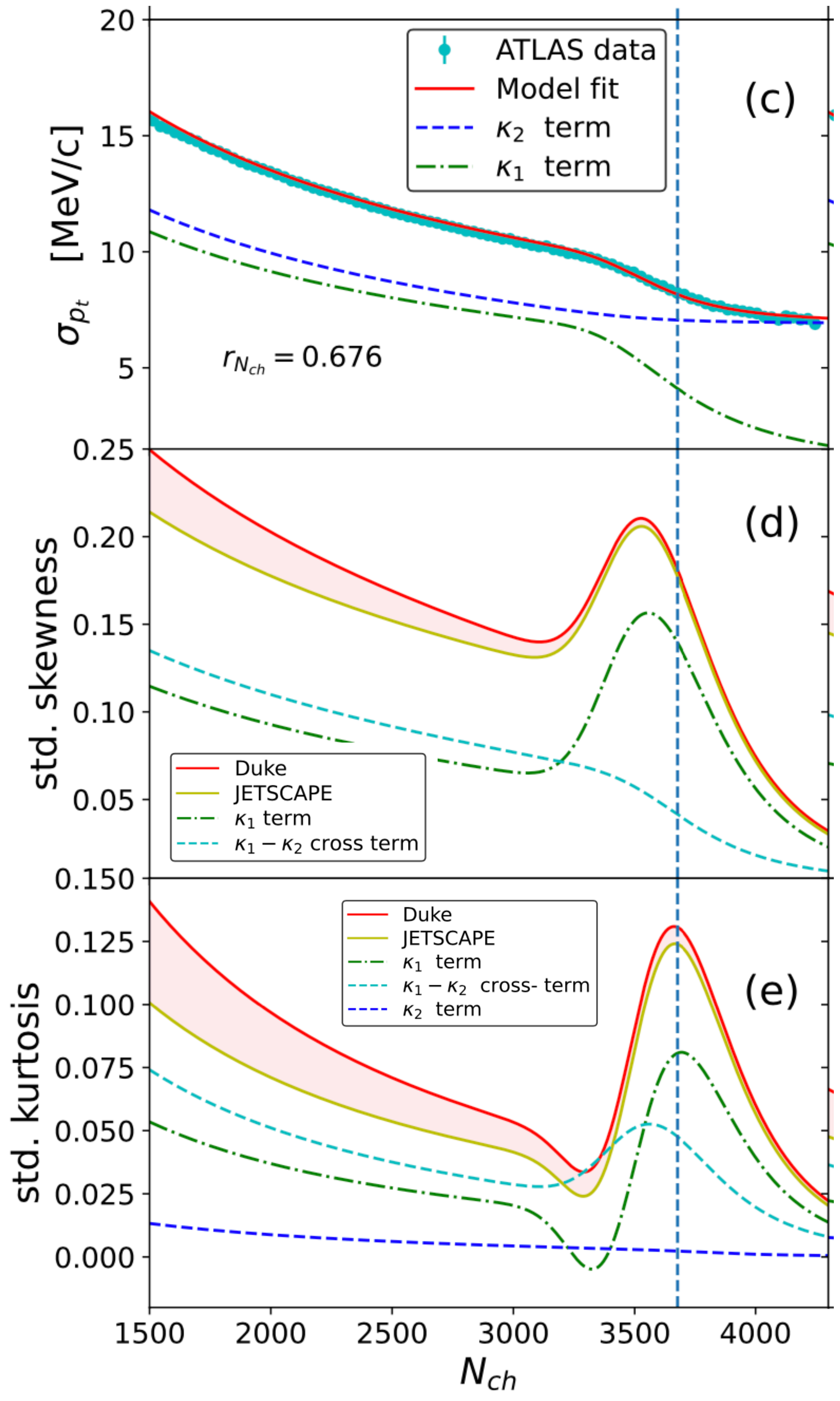

Transverse momentum fluctuations

The fluctuations of the event-by-event mean transverse momentum, $[p_{\mathrm{T}}]$, arise from two sources:

[R. Samanta et al., PRC 108 (2023) 024908]
[R. Samanta et al., PRC 109 (2024) L051902]

Geometrical fluctuations

- Radial flow: hydrodynamic response of $[p_{\mathrm{T}}]$ to the inverse size $1/R$
- At fixed multiplicity → radial flow fluctuations from fluctuations of inverse size

$\delta b \to 0$

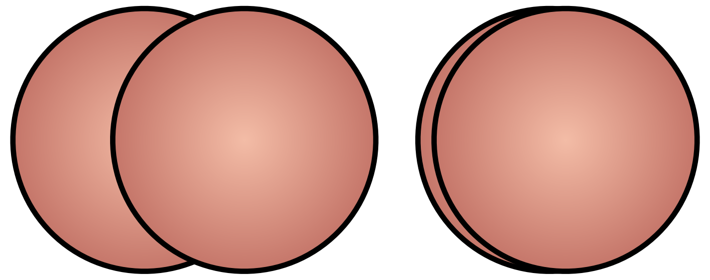

Intrinsic fluctuations

At fixed impact parameter *b*

- Quantum fluctuations in wave function of incoming nuclei
- Thermal fluctuations of the QGP

2D Gaussian model of $[p_{\mathrm{T}}]$ and N_{ch} fluctuations predicts abrupt changes of the higher-order $[p_{\mathrm{T}}]$ fluctuations with vanishing impact parameter fluctuations

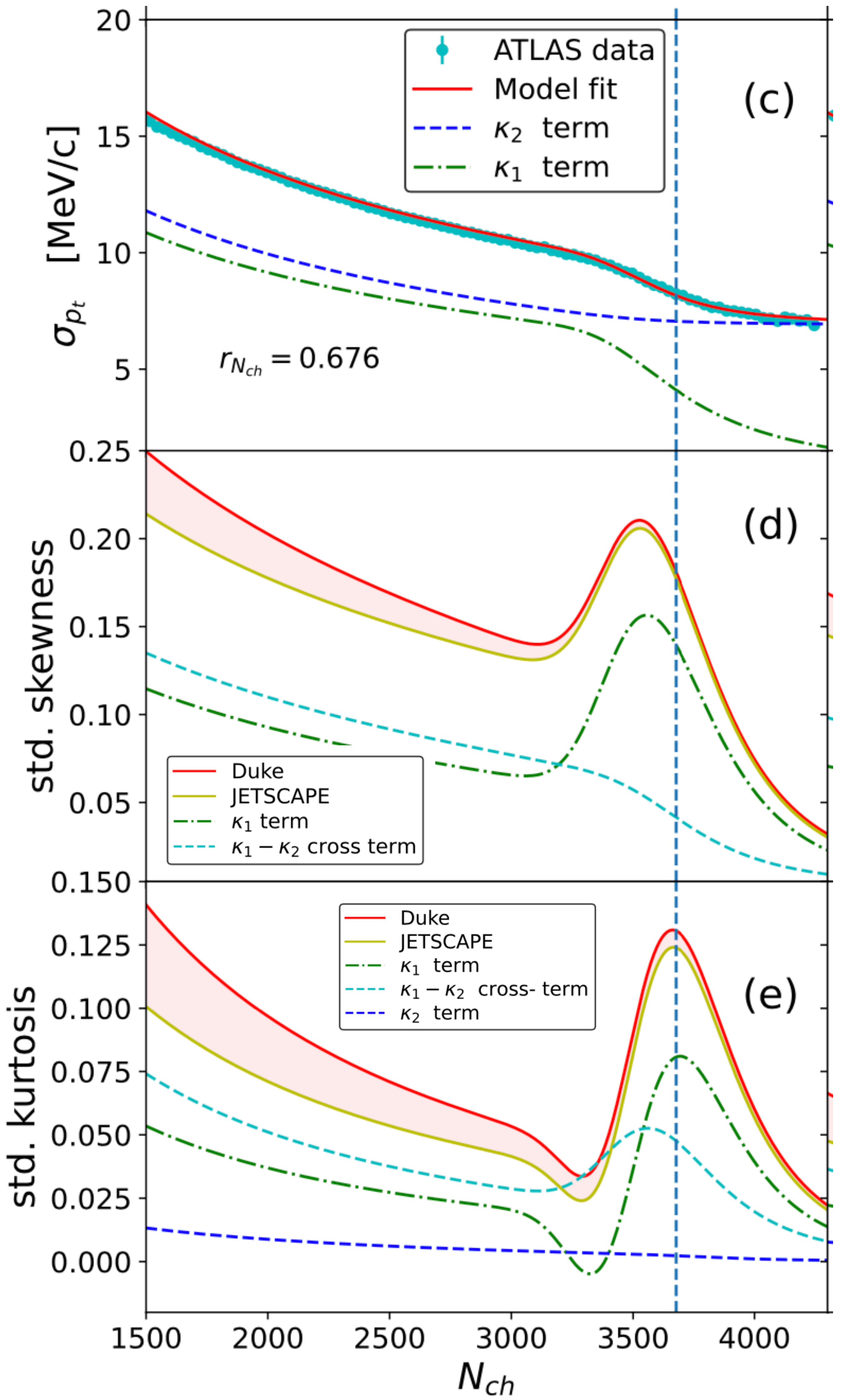

Measured quantities

Mean

From fully corrected spectra

$\langle p_{\mathrm{T}} \rangle$ extrapolated to $p_{\mathrm{T}} = 0$ with Levy-Tsallis parametrisation

Measured quantities

Mean

From fully corrected spectra

$\langle p_\mathrm{T} \rangle$ extrapolated to $p_\mathrm{T} = 0$ with Levy-Tsallis parametrisation

Variance

Normalised

$$k_2 = \frac{c_2}{\langle [p_\mathrm{T}^{(2)}] \rangle}$$

c_n = n$^{\mathrm{th}}$-order multi-particle $[p_\mathrm{T}]$-cumulant

$[p_\mathrm{T}^{(n)}]$ = n$^{\mathrm{th}}$-order multi-particle $[p_\mathrm{T}]$-moment

Measured quantities

Mean

From fully corrected spectra

$\langle p_{\mathrm{T}} \rangle$ extrapolated to $p_{\mathrm{T}} = 0$ with Levy-Tsallis parametrisation

Variance

Normalised

$$k_2 = \frac{c_2}{\langle [p_{\mathrm{T}}^{(2)}] \rangle}$$

Skewness

Normalised

$$k_3 = \frac{c_3}{\langle [p_{\mathrm{T}}^{(3)}] \rangle}$$

Standardised

$$\gamma_{\langle [p_{\mathrm{T}}] \rangle} = \frac{c_3}{c_2^{3/2}}$$

Intensive

$$\Gamma_{\langle [p_{\mathrm{T}}] \rangle} = \frac{c_3 \cdot \langle [p_{\mathrm{T}}] \rangle}{c_2^2}$$

c_n = n$^{\mathrm{th}}$-order multi-particle $[p_{\mathrm{T}}]$-cumulant

$[p_{\mathrm{T}}^{(n)}]$ = n$^{\mathrm{th}}$-order multi-particle $[p_{\mathrm{T}}]$-moment

Skewness

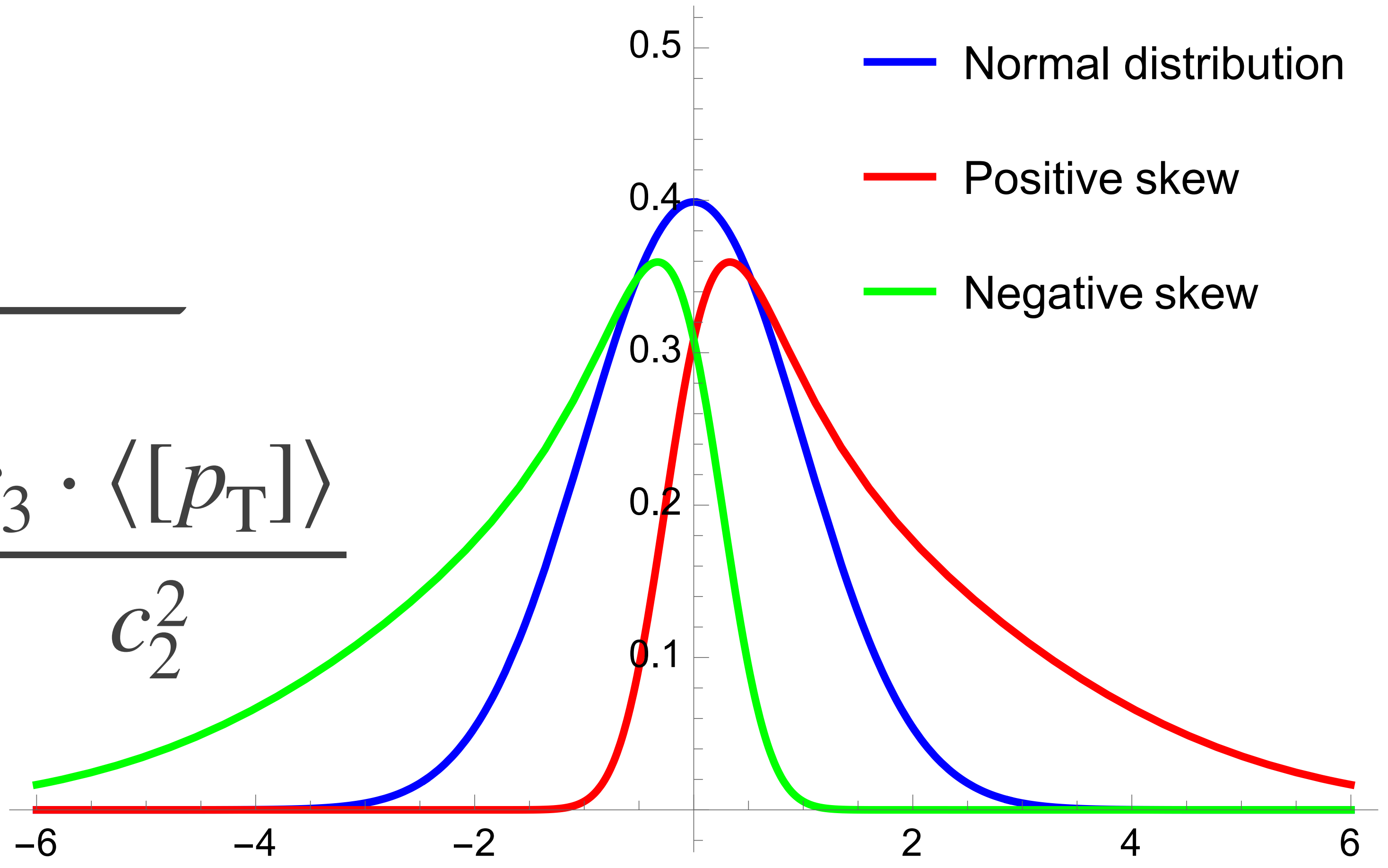

Measured quantities

c_n = n$^{\text{th}}$-order multi-particle $[p_\text{T}]$-cumulant

$[p_\text{T}^{(n)}]$ = n$^{\text{th}}$-order multi-particle $[p_\text{T}]$-moment

Mean

From fully corrected spectra

$\langle p_\text{T}\rangle$ extrapolated to $p_\text{T}=0$ with Levy-Tsallis parametrisation

Variance

Normalised

$$k_2 = \frac{c_2}{\langle [p_\text{T}^{(2)}]\rangle}$$

Skewness

Normalised

$$k_3 = \frac{c_3}{\langle [p_\text{T}^{(3)}]\rangle}$$

Standardised

$$\gamma_{\langle [p_\text{T}]\rangle} = \frac{c_3}{c_2^{3/2}}$$

Intensive

$$\Gamma_{\langle [p_\text{T}]\rangle} = \frac{c_3 \cdot \langle [p_\text{T}]\rangle}{c_2^2}$$

Skewness

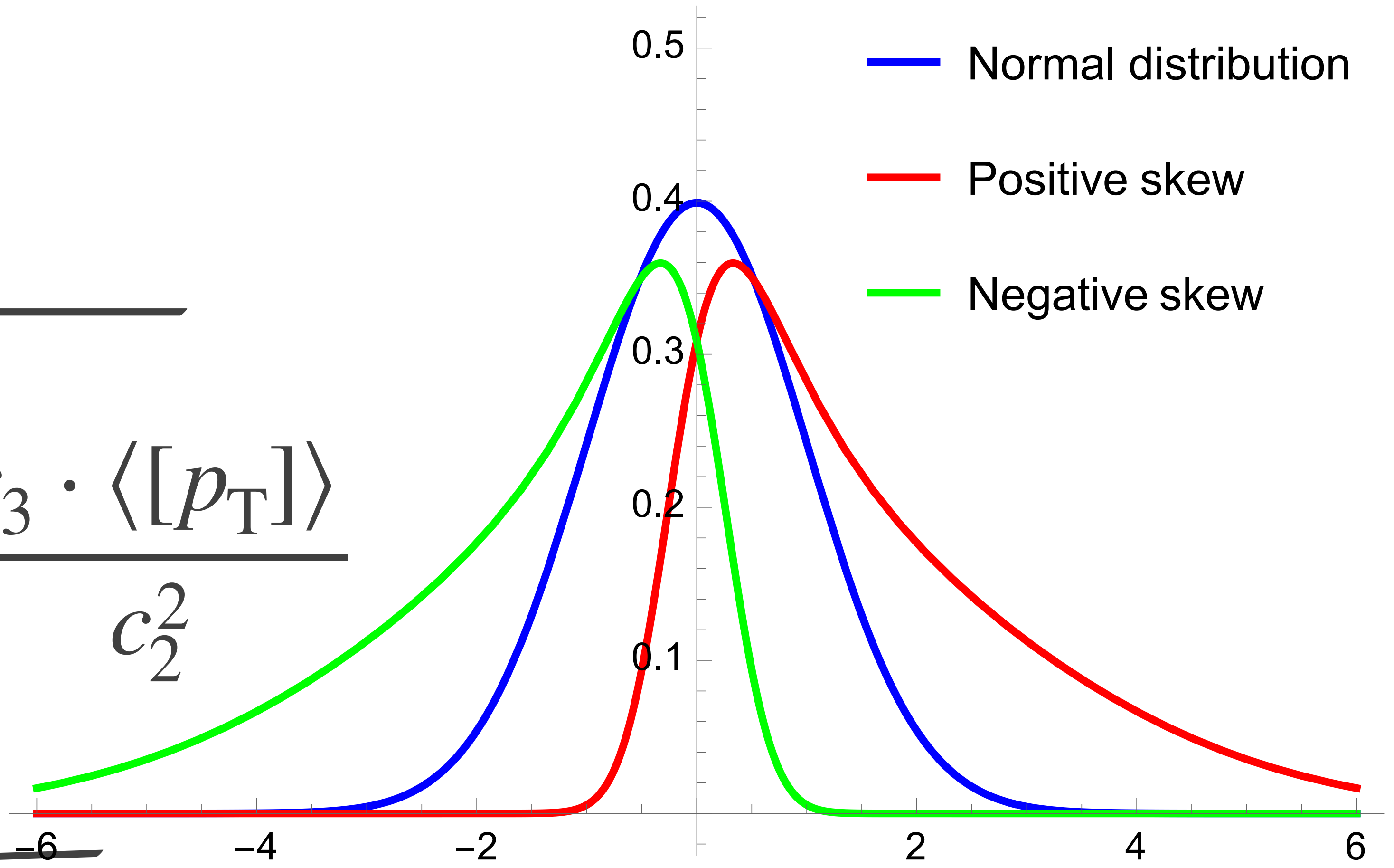

Kurtosis

$$\kappa_{\langle [p_\text{T}]\rangle} = \frac{c_4 + 3c_2^2}{c_2^2}$$

Kurtosis

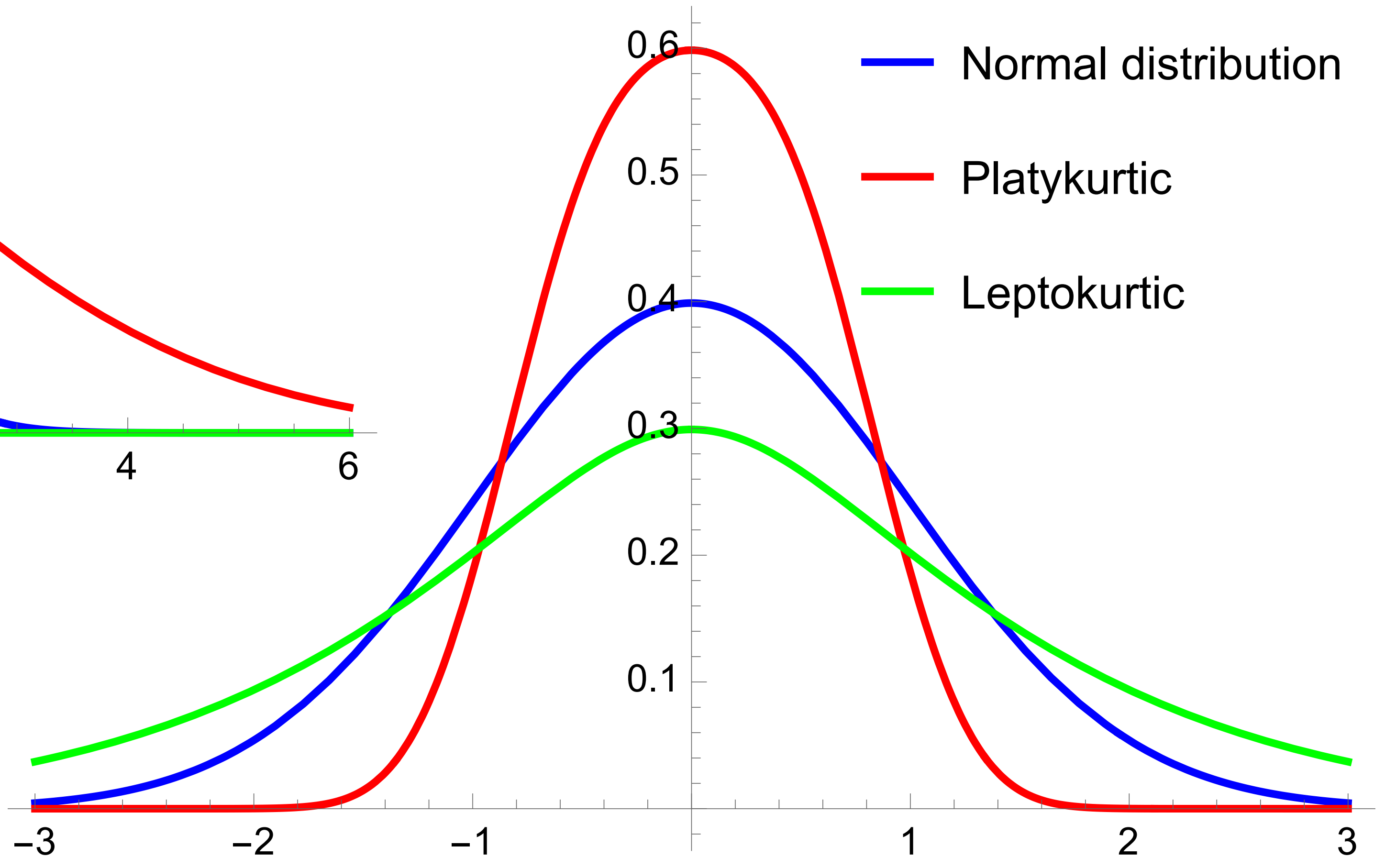

Mean transverse momentum

Correlation between $\langle p_T \rangle$ and N_{ch} fitted with parametrisation
[F. Gardim et al., PLB 809 (2020) 135749]

$$\langle p_T \rangle / \langle p_T \rangle^{ref} = \left(\frac{N^*_{ch}}{f(N^*_{ch}, N^*_{ch,knee}, \sigma_0)} \right)^{c_s^2}$$

Gaussian fluctuations of N_{ch} as function of impact parameter

where $N^*_{ch} = \langle dN_{ch}/d\eta \rangle / \langle dN_{ch}/d\eta \rangle^{ref}$

$N^*_{ch,knee}$ and σ_0 obtained from fit to multiplicity distribution
[S. J. Das et al., PRC 97, 014905 (2018)]

NEW

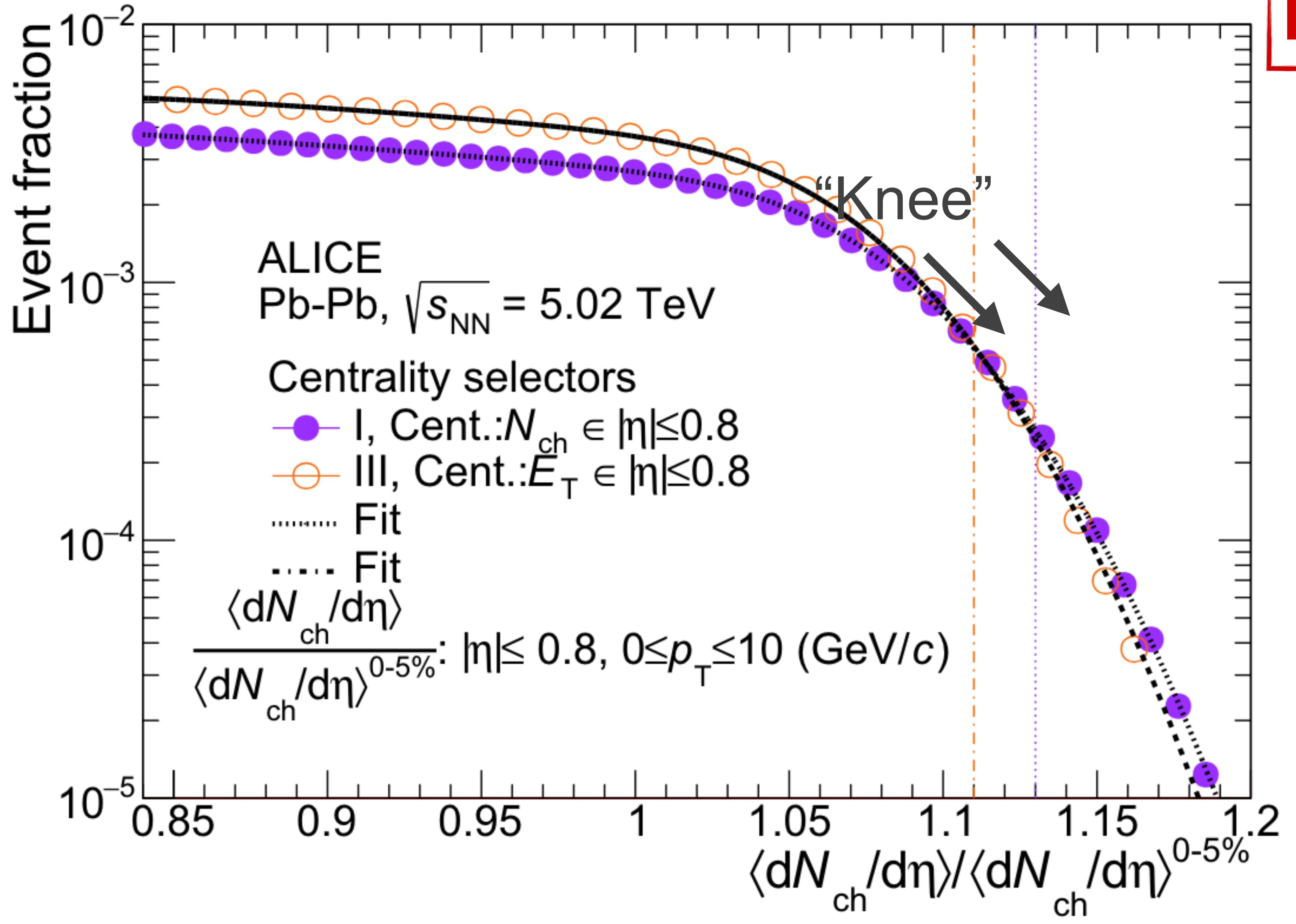

Mean transverse momentum

Correlation between $\langle p_T \rangle$ and N_{ch} fitted with parametrisation [F. Gardim et al., PLB 809 (2020) 135749]

$$\langle p_T \rangle / \langle p_T \rangle^{ref} = \left(\frac{N^*_{ch}}{f(N^*_{ch}, N^*_{ch,knee}, \sigma_0)} \right)^{c_s^2}$$

Gaussian fluctuations of N_{ch} as function of impact parameter

where $N^*_{ch} = \langle dN_{ch}/d\eta \rangle / \langle dN_{ch}/d\eta \rangle^{ref}$

$N^*_{ch,knee}$ and σ_0 obtained from fit to multiplicity distribution [S. J. Das et al., PRC 97, 014905 (2018)]

NEW

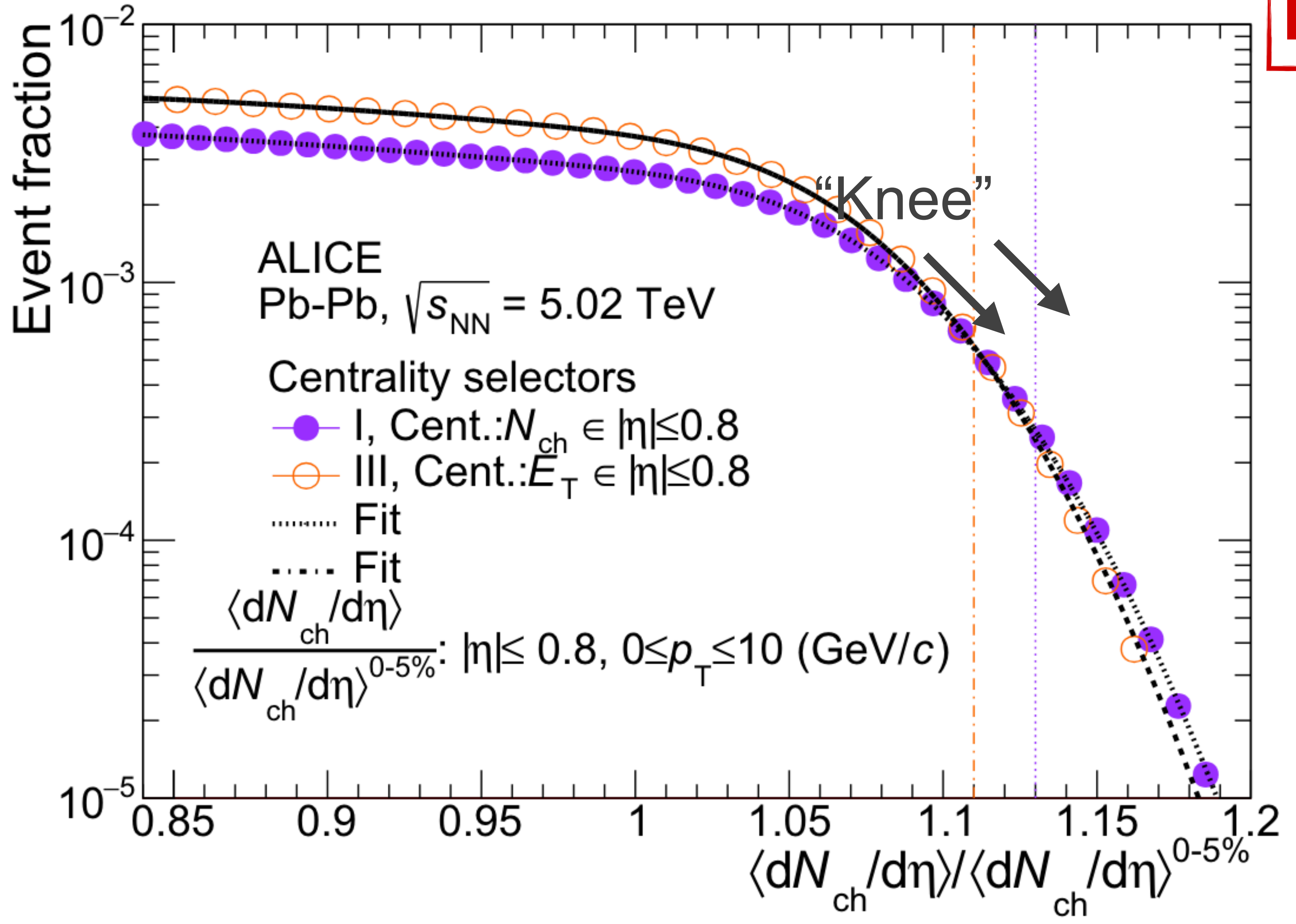

Below the knee

$$\langle p_T \rangle / \langle p_T \rangle^{ref} \approx 1$$

Mean transverse momentum

Correlation between $\langle p_T \rangle$ and N_{ch} fitted with parametrisation
[F. Gardim et al., PLB 809 (2020) 135749]

$$\langle p_T \rangle / \langle p_T \rangle^{ref} = \left(\frac{N^*_{ch}}{f(N^*_{ch}, N^*_{ch,knee}, \sigma_0)} \right)^{c_s^2}$$

Gaussian fluctuations of N_{ch} as function of impact parameter

where $N^*_{ch} = \langle dN_{ch}/d\eta \rangle / \langle dN_{ch}/d\eta \rangle^{ref}$

$N^*_{ch,knee}$ and σ_0 obtained from fit to multiplicity distribution
[S. J. Das et al., PRC 97, 014905 (2018)]

NEW

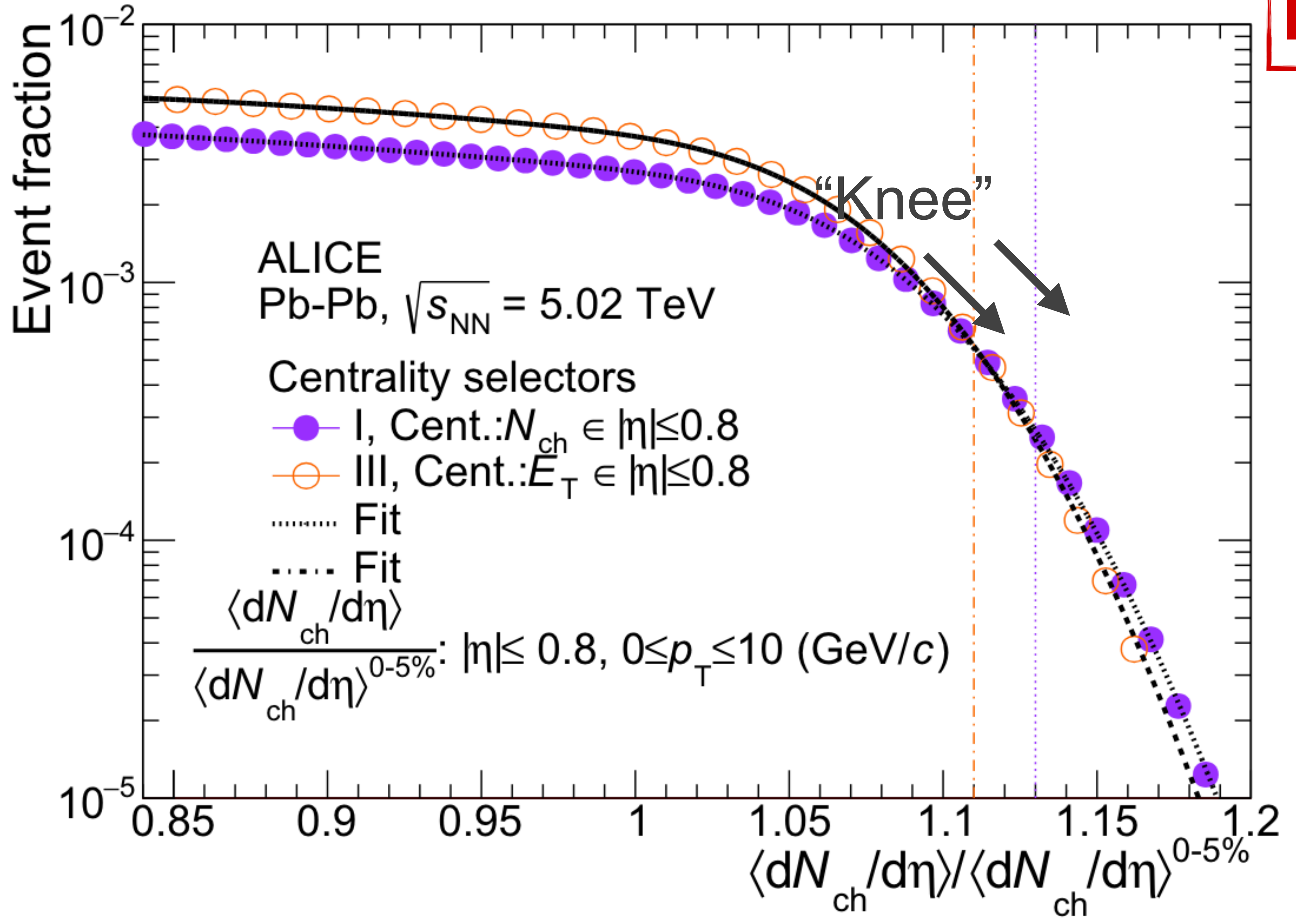

Below the knee

$$\langle p_T \rangle / \langle p_T \rangle^{ref} \approx 1$$

Above the knee

$$\langle p_T \rangle / \langle p_T \rangle^{ref} \propto \left(\frac{N^*_{ch}}{N^*_{ch,knee}} \right)^{c_s^2}$$

The ALICE experiment

Relevant subdetectors:

Inner Tracking System (ITS)

Vertex identification, tracking

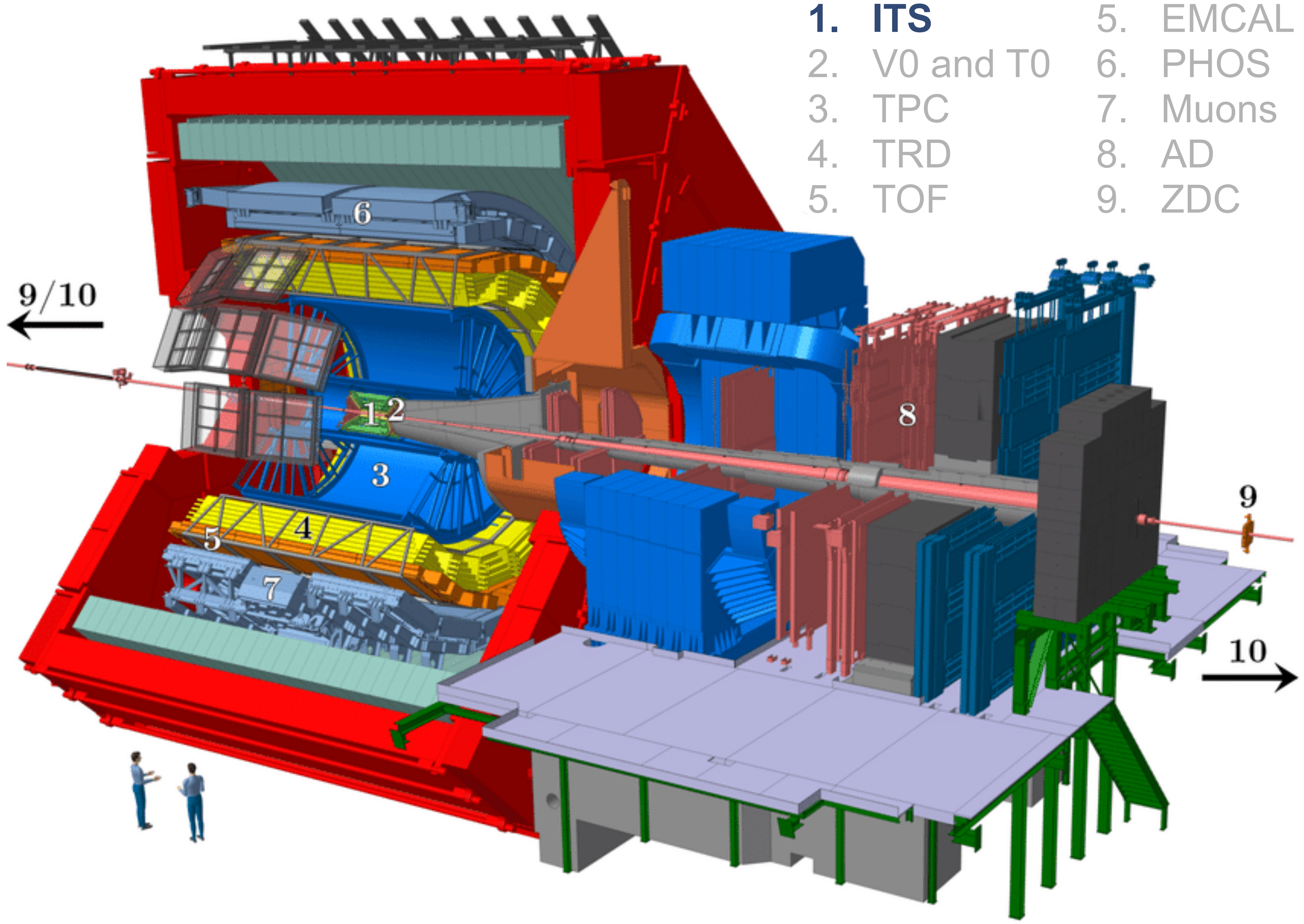

Collision system:

Pb–Pb at $\sqrt{s_{\mathrm{NN}}} = 5.02$ TeV

Charged-particle **multiplicity** down to 30 MeV/c with ITS tracklets in ALICE

Tracklet: track segments joining hits in two innermost ITS layers

The ALICE experiment

Relevant subdetectors:

Inner Tracking System (ITS)

Vertex identification, tracking

Time-Projection Chamber (TPC)

Tracking, particle identification

1. ITS
2. V0 and T0
3. **TPC**
4. TRD
5. TOF
5. EMCAL
6. PHOS
7. Muons
8. AD
9. ZDC

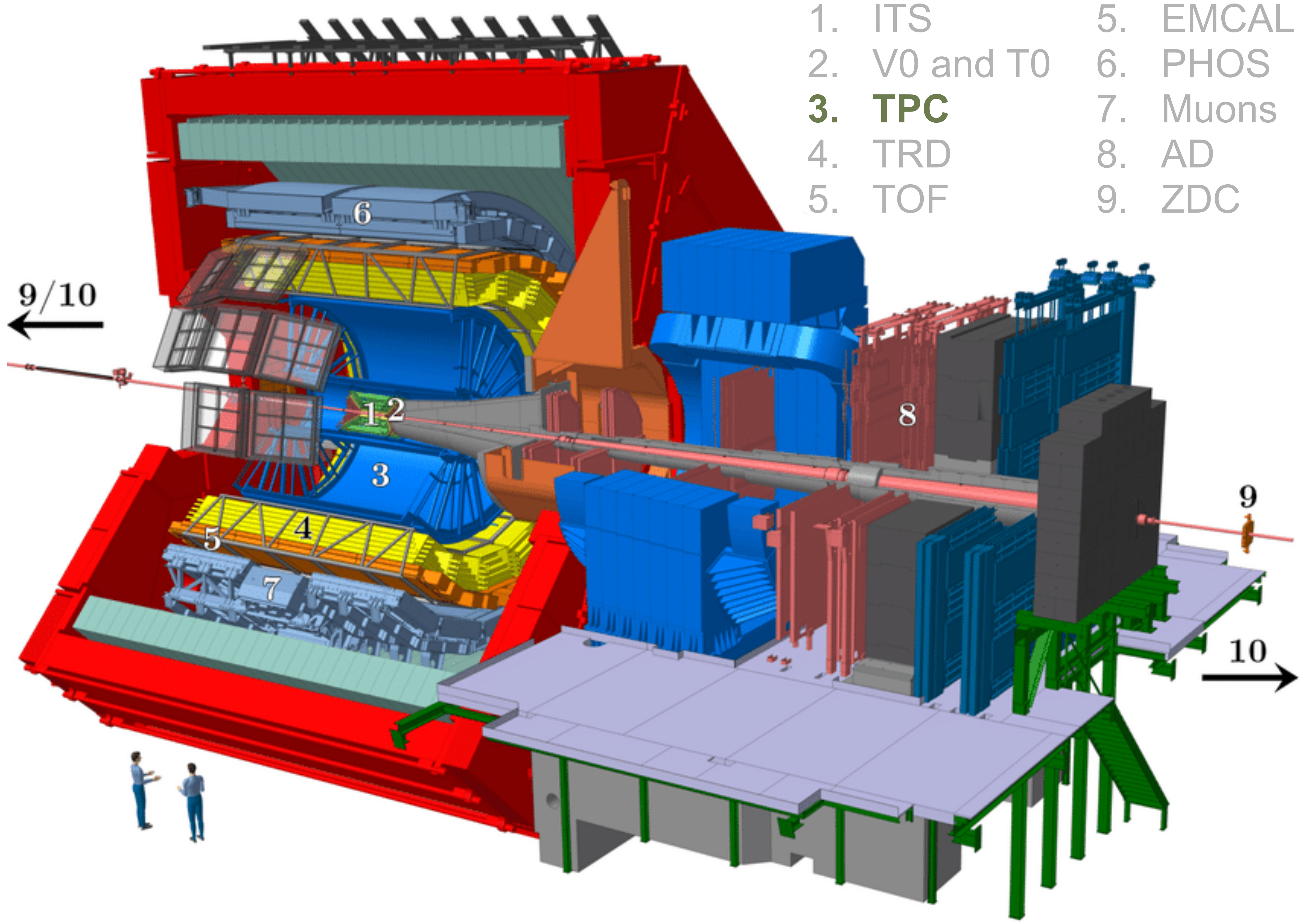

Collision system:

Pb−Pb at $\sqrt{s_{\mathrm{NN}}} = 5.02$ TeV

Charged-particle **multiplicity** down to 30 MeV/c with ITS tracklets in ALICE

Tracklet: track segments joining hits in two innermost ITS layers

The ALICE experiment

Relevant subdetectors:

Inner Tracking System (ITS)

Vertex identification, tracking

Time-Projection Chamber (TPC)

Tracking, particle identification

V0A ($2.8 < \eta < 5.1$) and V0C ($-3.7 < \eta < -1.7$)

Multiplicity and centrality estimation

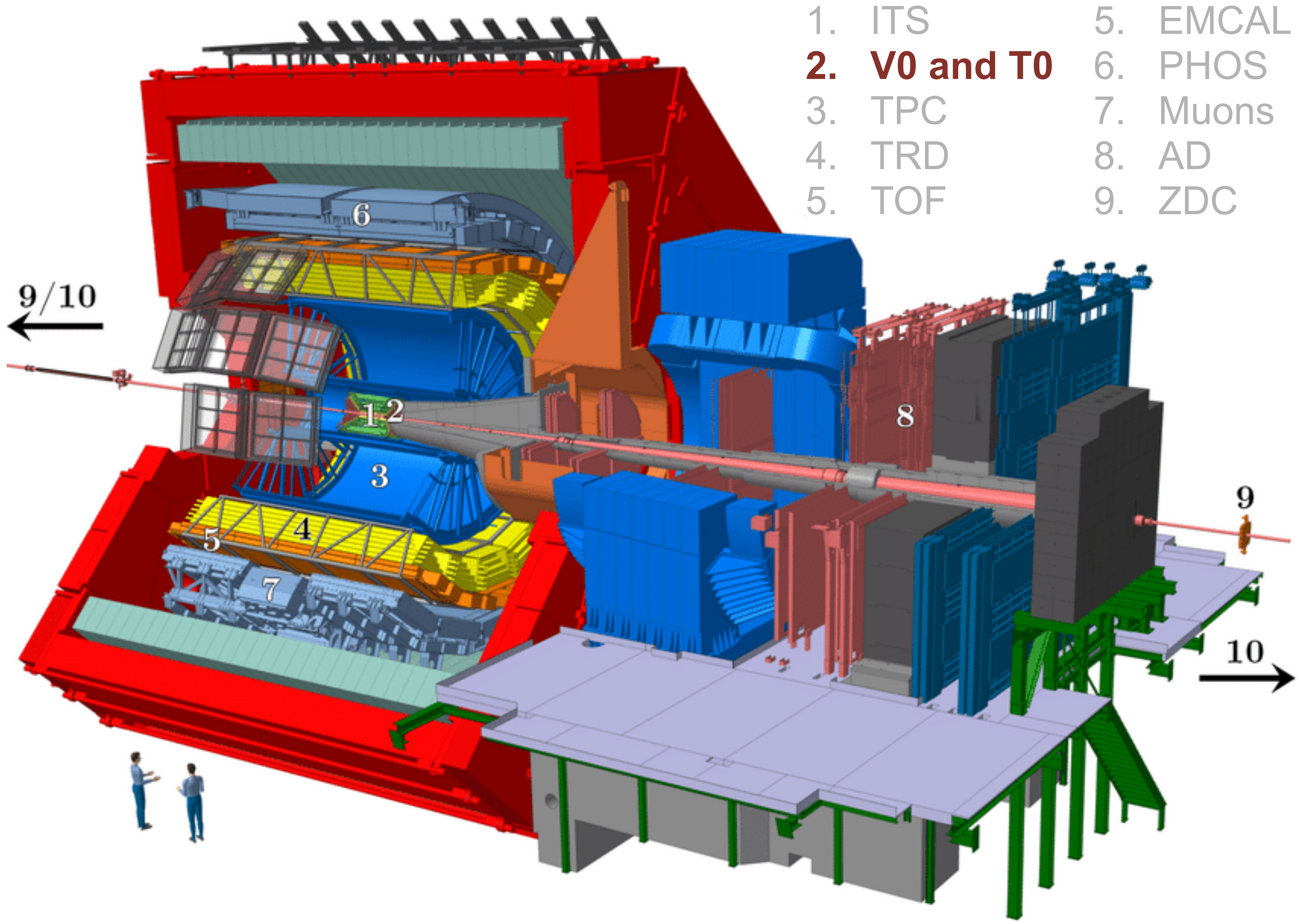

Collision system:

Pb–Pb at $\sqrt{s_{\mathrm{NN}}} = 5.02$ TeV

Charged-particle **multiplicity** down to 30 MeV/*c* with ITS tracklets in ALICE

Tracklet: track segments joining hits in two innermost ITS layers

Extracting the speed of sound

Extraction of c_s^2 depends on the centrality determination

- Forward vs. midrapidity
- ITS tracklets vs full tracks
- E_T vs N_{ch}

Decreased c_s^2 using forward centrality determination

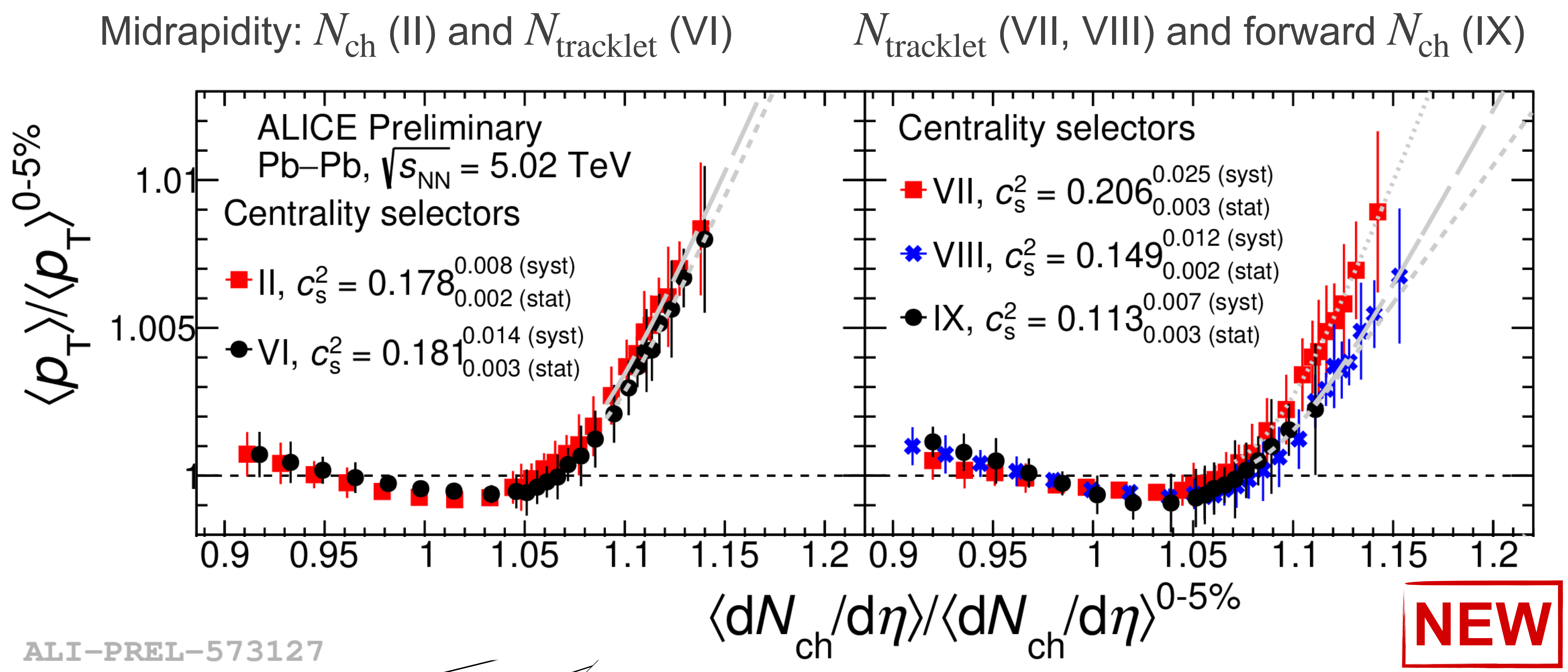

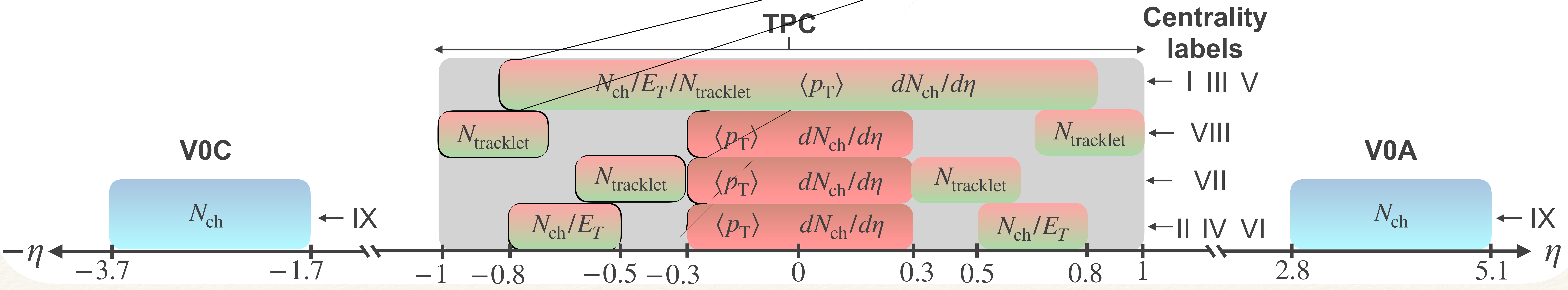

Extracting the speed of sound

Extraction of c_s^2 depends on the centrality determination

- Forward vs. midrapidity
- ITS tracklets vs full tracks
- E_T vs N_{ch}

Decreased c_s^2 using forward centrality determination

Increased c_s^2 using E_T

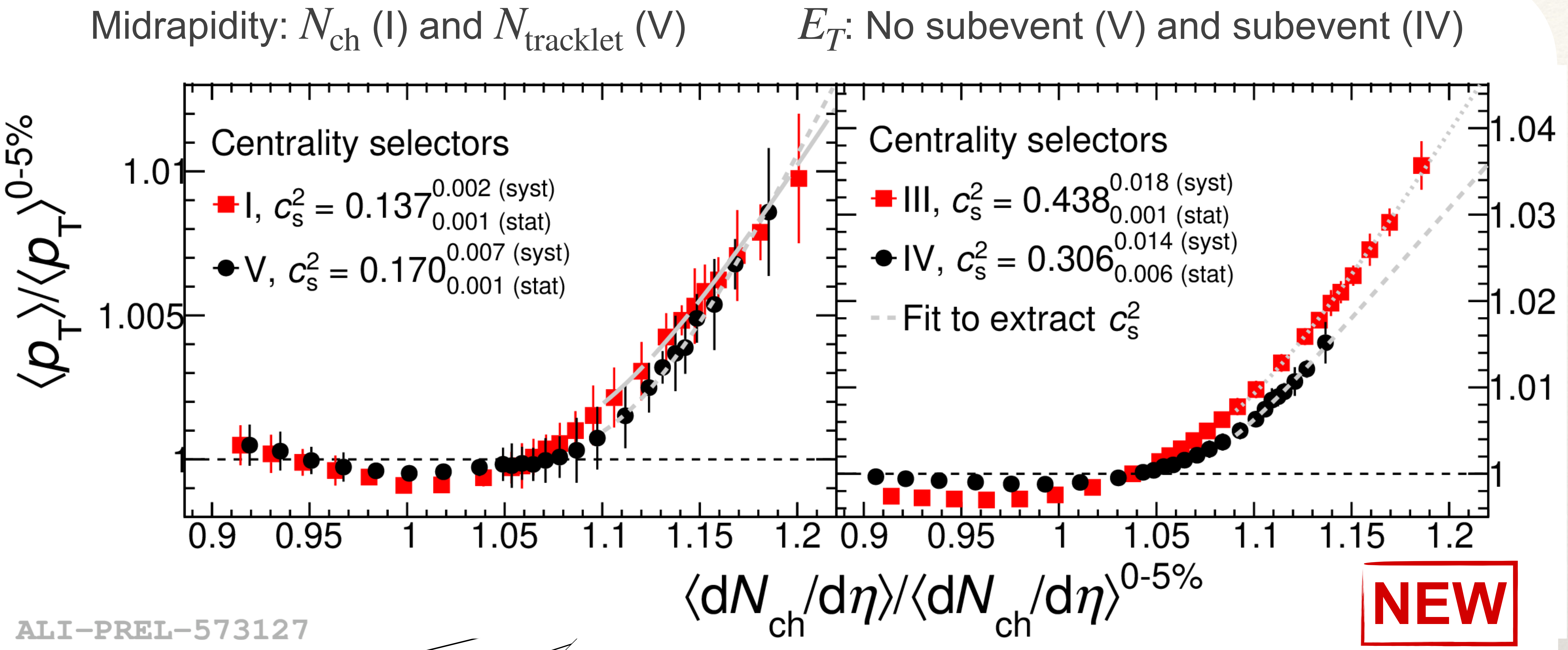

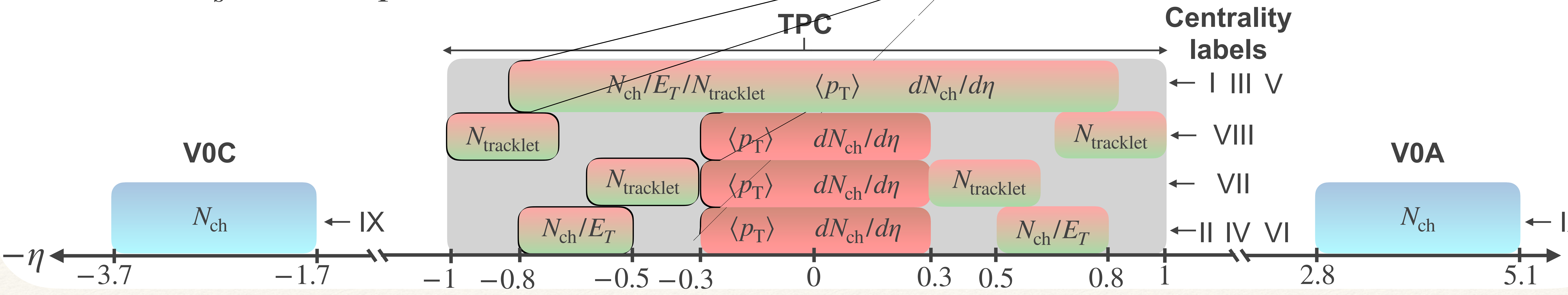

Speed of sound as function of η-gap

NEW

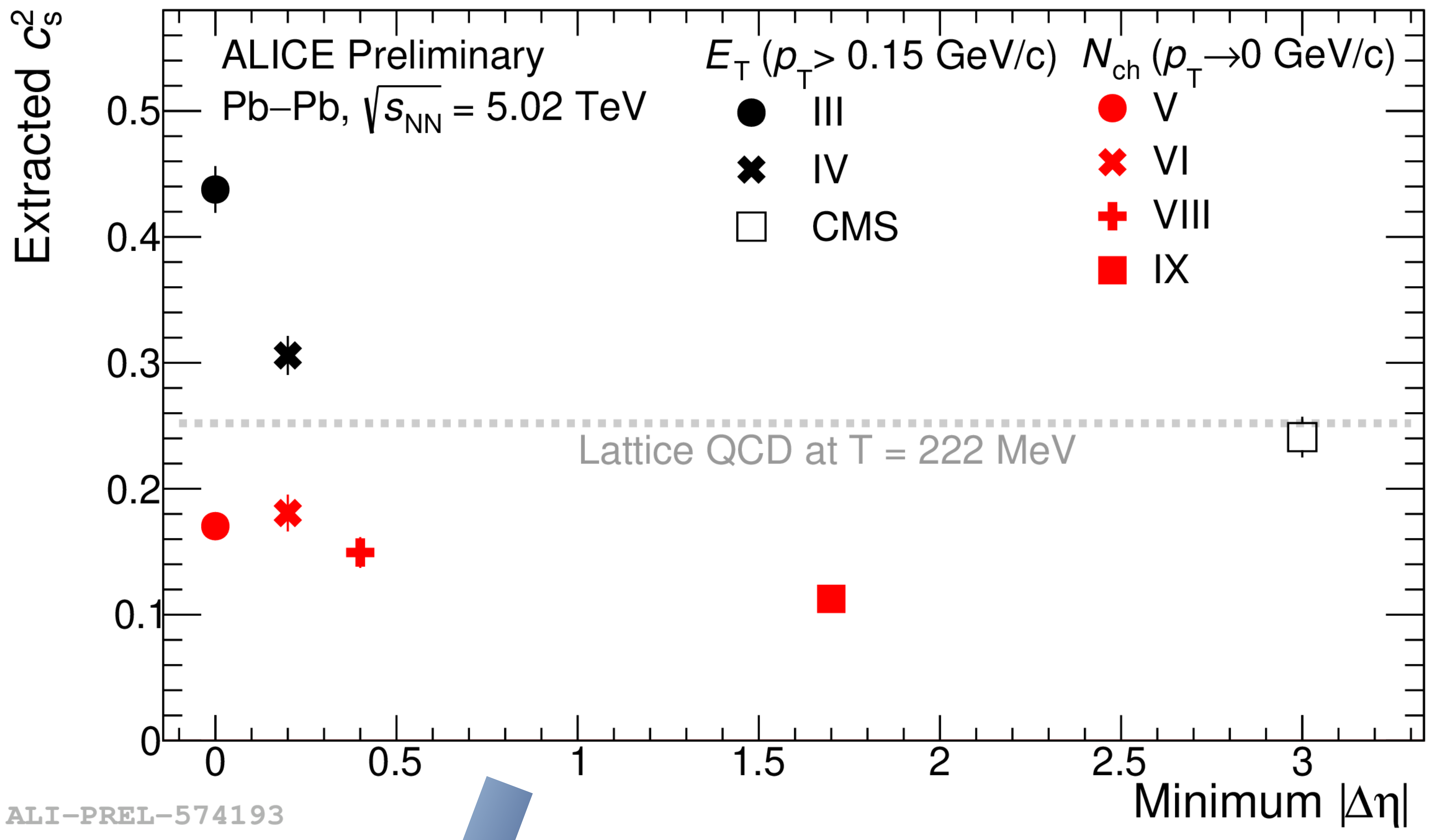

Observable	Label	Centrality estimation	$\langle p_T \rangle$ and $\langle dN_{ch}/d\eta \rangle$	η gap
N_{ch} in TPC	I	$\lvert\eta\rvert \le 0.8$	$\lvert\eta\rvert \le 0.8$	0
	II	$0.5 \le \lvert\eta\rvert \le 0.8$	$\lvert\eta\rvert \le 0.3$	0.3
E_T in TPC	III	$\lvert\eta\rvert \le 0.8$	$\lvert\eta\rvert \le 0.8$	0
	IV	$0.5 \le \lvert\eta\rvert \le 0.8$	$\lvert\eta\rvert \le 0.3$	0.3
$N_{tracklets}$ in SPD	V	$\lvert\eta\rvert \le 0.8$	$\lvert\eta\rvert \le 0.8$	0
	VI	$0.5 \le \lvert\eta\rvert \le 0.8$	$\lvert\eta\rvert \le 0.3$	0.3
	VII	$0.3 < \lvert\eta\rvert \le 0.6$	$\lvert\eta\rvert \le 0.3$	0
	VIII	$0.7 \le \lvert\eta\rvert \le 1$	$\lvert\eta\rvert \le 0.3$	0.4
N_{ch} in V0	IX	$-3.7 < \eta < -1.7 + 2.8 < \eta < 5.1$	$\lvert\eta\rvert \le 0.8$	1.7

Summary plot of extracted c_s^2 with different centrality estimators and various η separations between particles used for $\langle p_T \rangle$ and centrality

Variance of $[p_T]$ in UCC

- Variances measured as a function of multiplicity determined from both midrapidity and forward rapidity

NEW

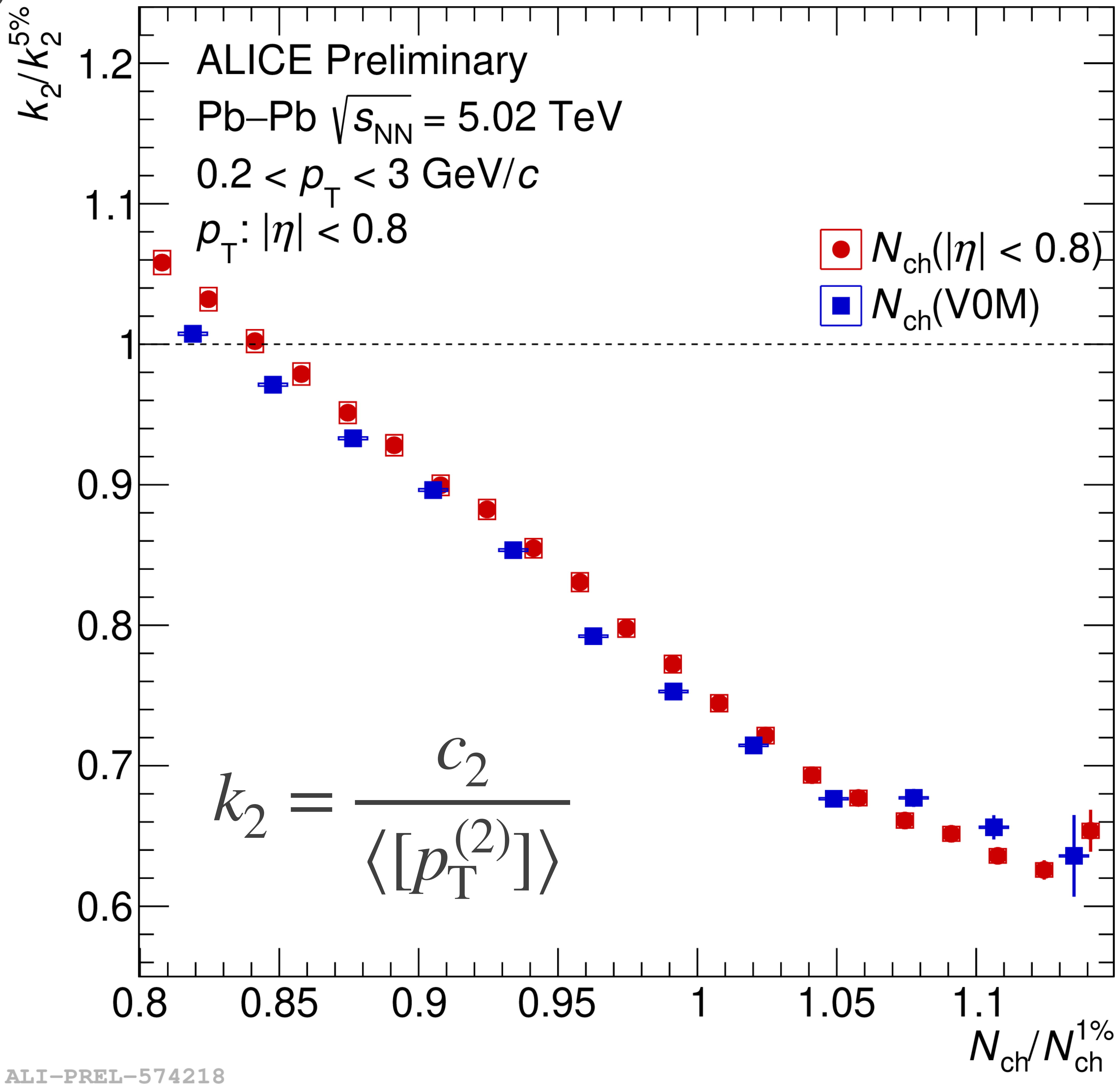

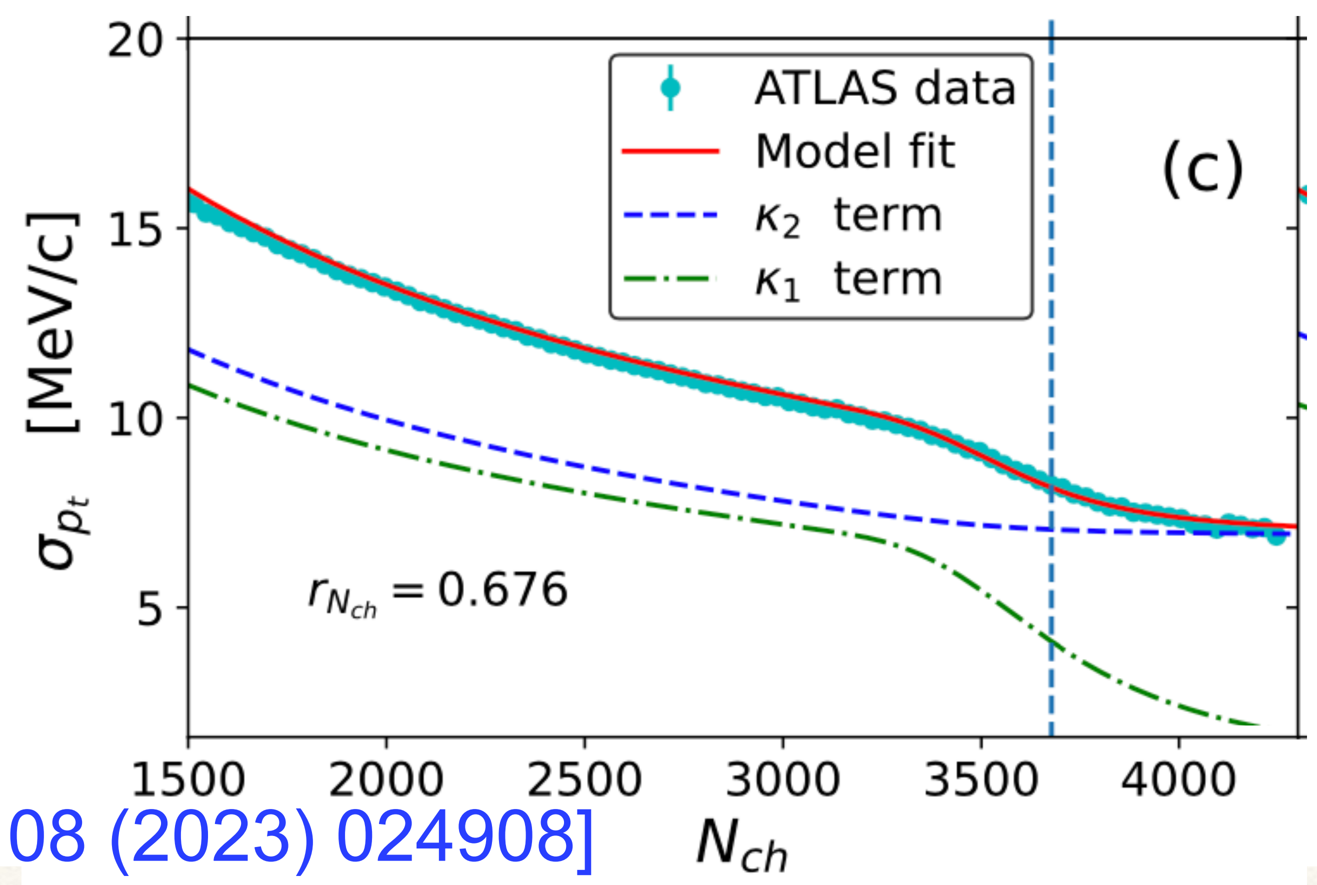

[R. Samanta et al., PRC 108 (2023) 024908]

Variance of $[p_\mathrm{T}]$ in UCC

- Variances measured as a function of multiplicity determined from both midrapidity and forward rapidity
- Independent sources picture (HIJING) : $\rightarrow k_2 \propto N_\mathrm{ch}^{-1}$
- Decrease of variance in UCC evidence of thermalisation of the medium

NEW

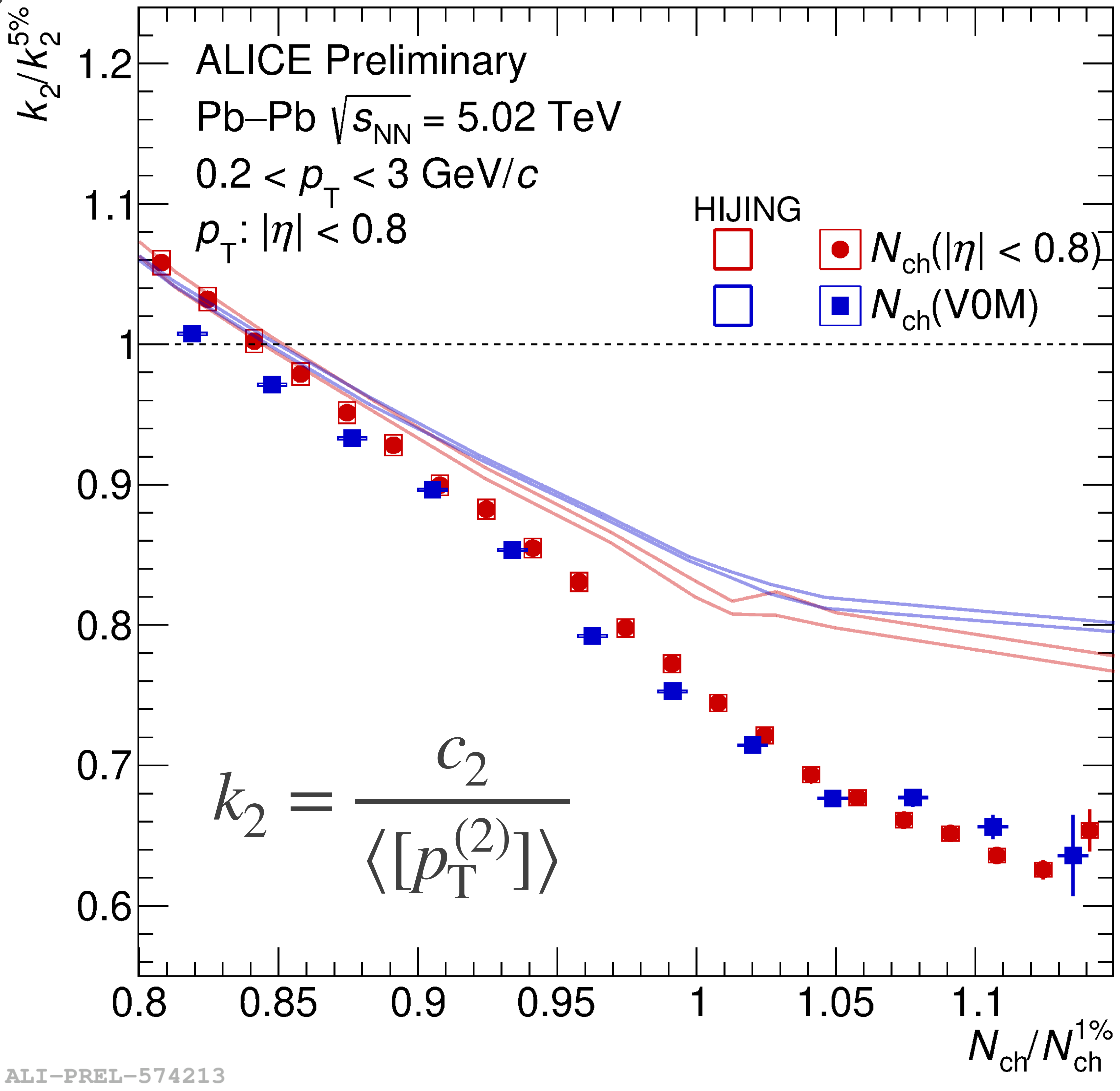

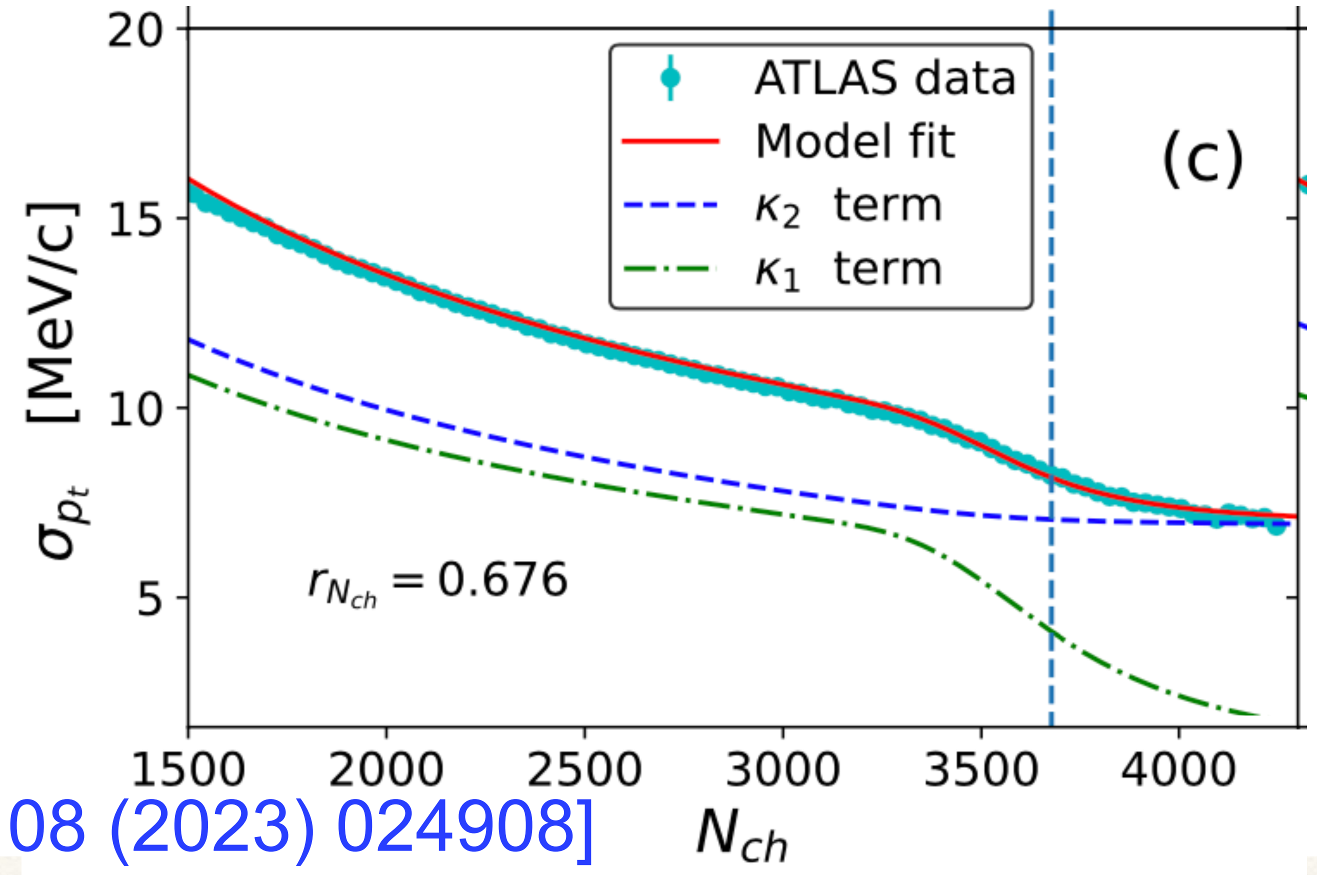

[R. Samanta et al., PRC 108 (2023) 024908]

Variance of $[p_T]$ in UCC

- Variances measured as a function of multiplicity determined from both midrapidity and forward rapidity
- Independent sources picture (HIJING) : $\rightarrow k_2 \propto N_{ch}^{-1}$
- Decrease of variance in UCC evidence of thermalisation of the medium
- Trajectum: good agreement with data

[G. Nijs and W. van der Schee, PLB 853 (2024) 138636]

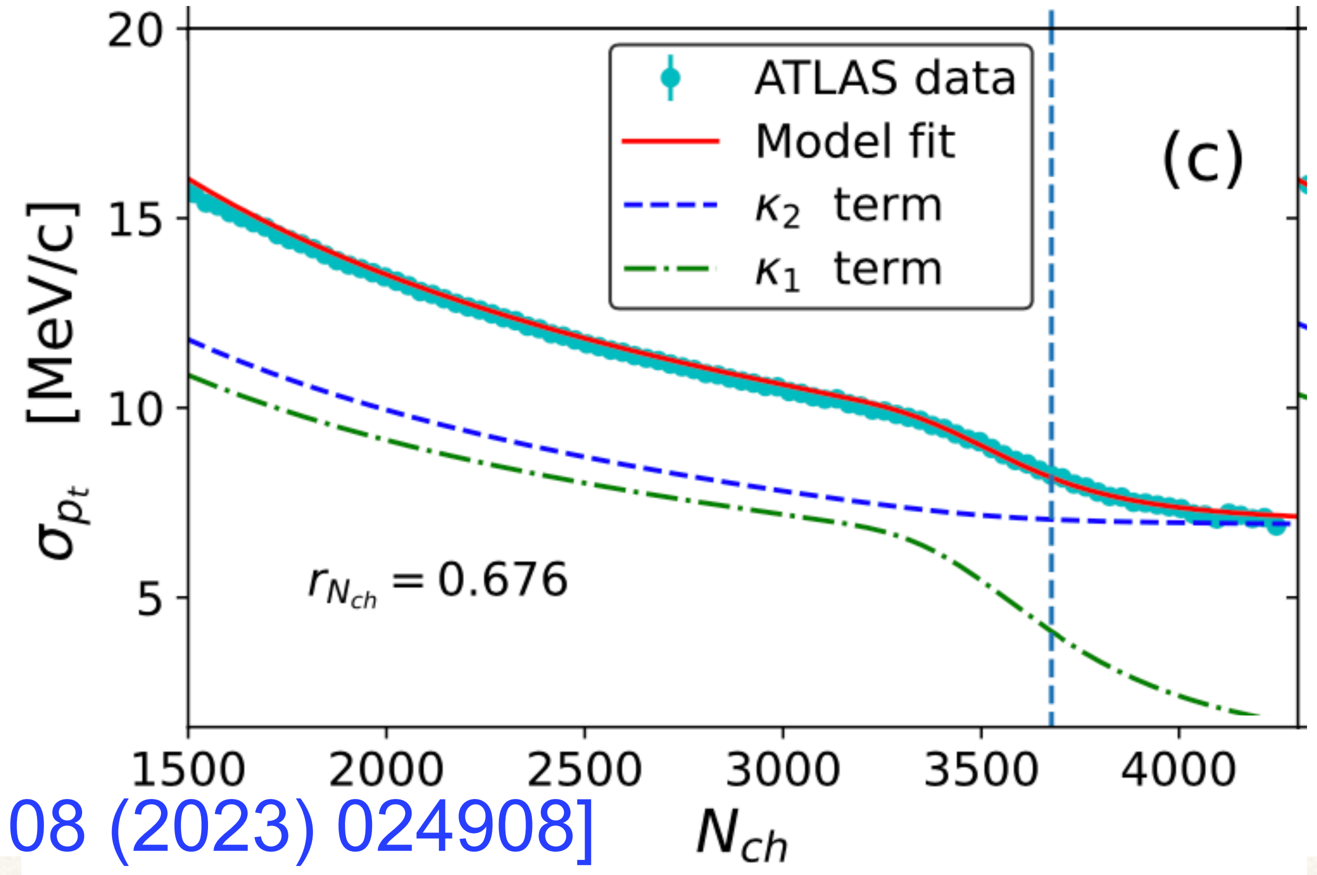

[R. Samanta et al., PRC 108 (2023) 024908]

NEW

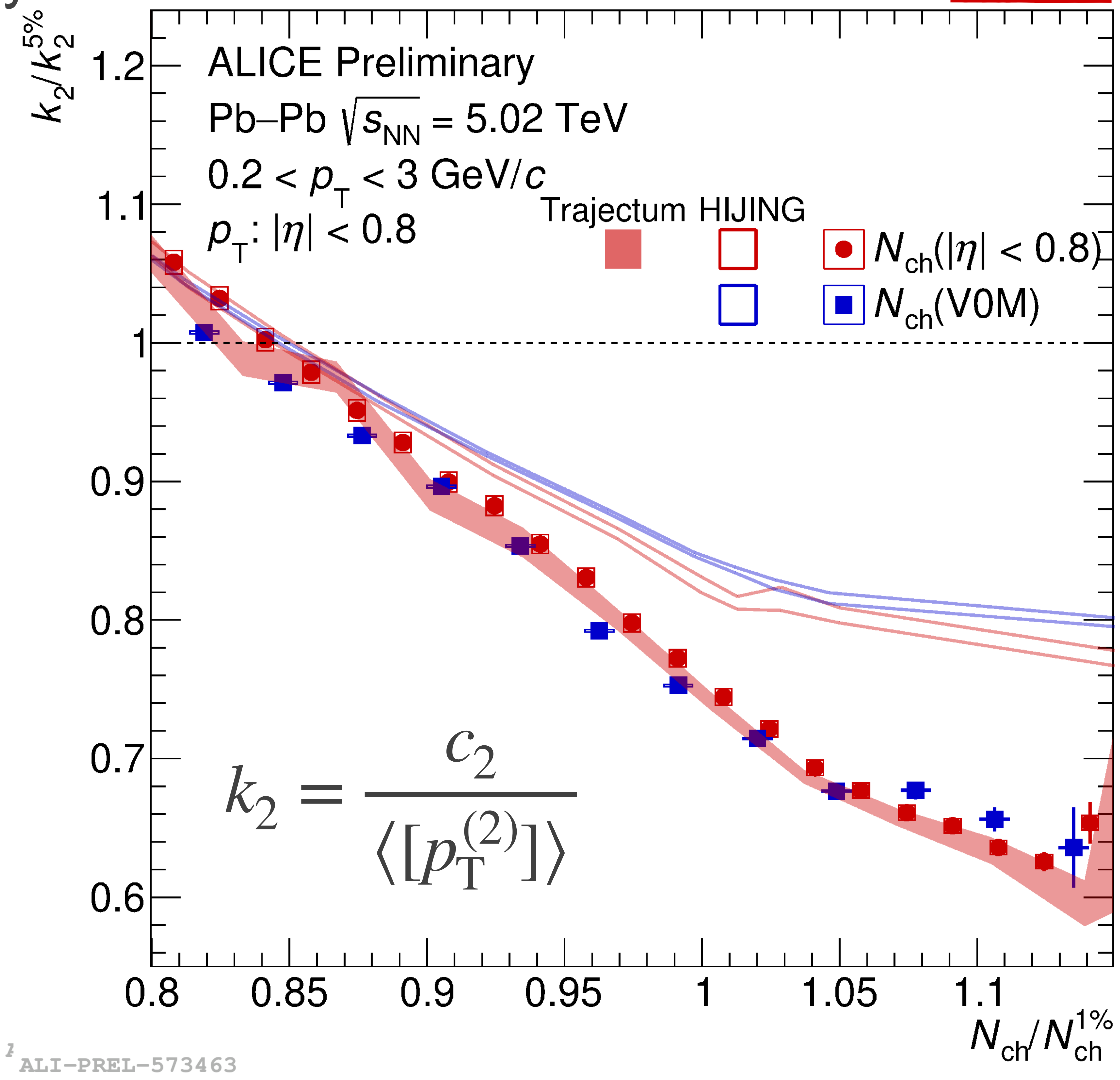

Skewness of $[p_T]$ in UCC

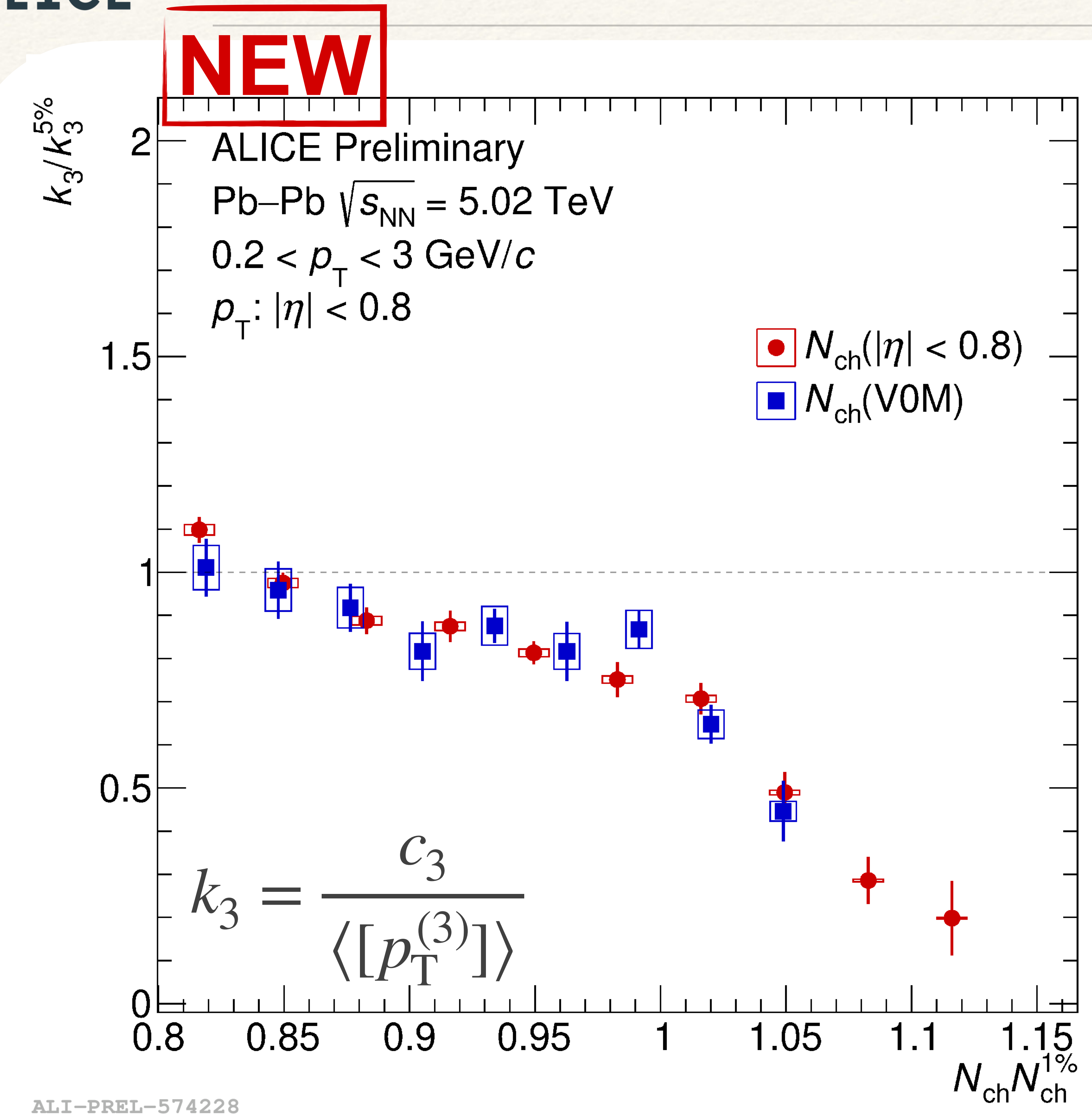

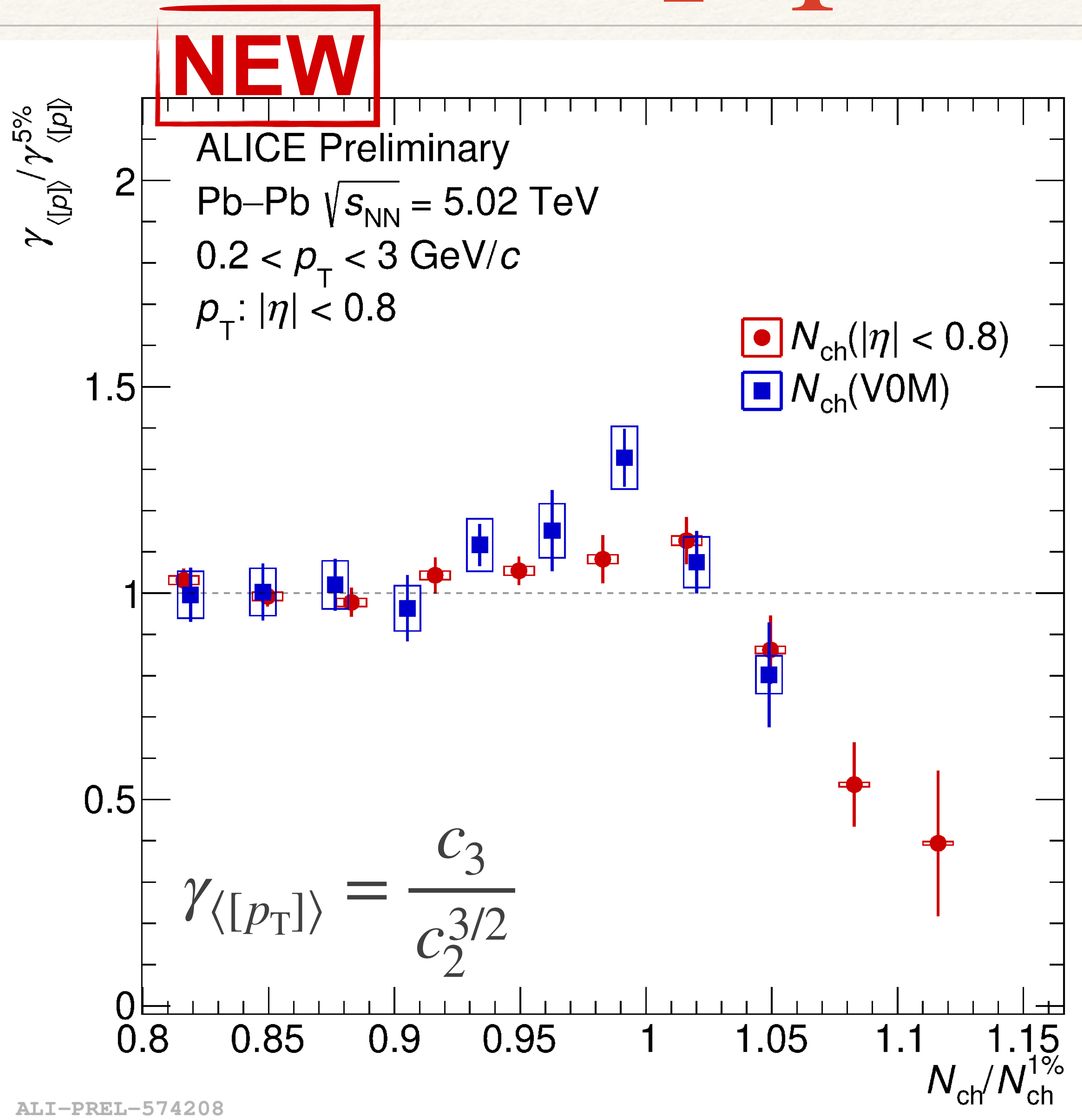

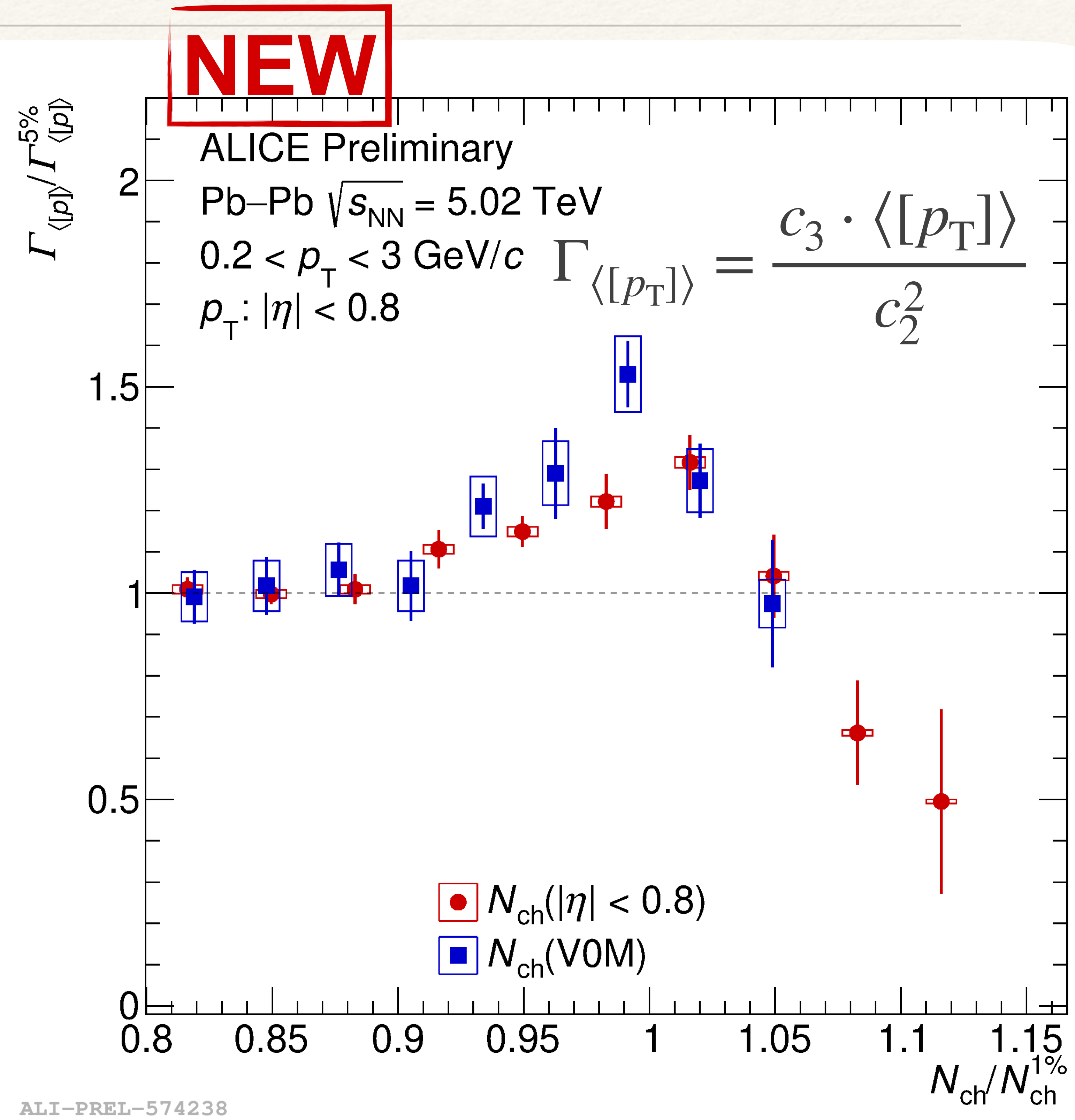

- Skewness behaviour depends on normalisation
- Interplay between skewness and variance in $\gamma_{\langle [p_T] \rangle}$ and $\Gamma_{\langle [p_T] \rangle}$
- Bump driven by geometrical fluctuations

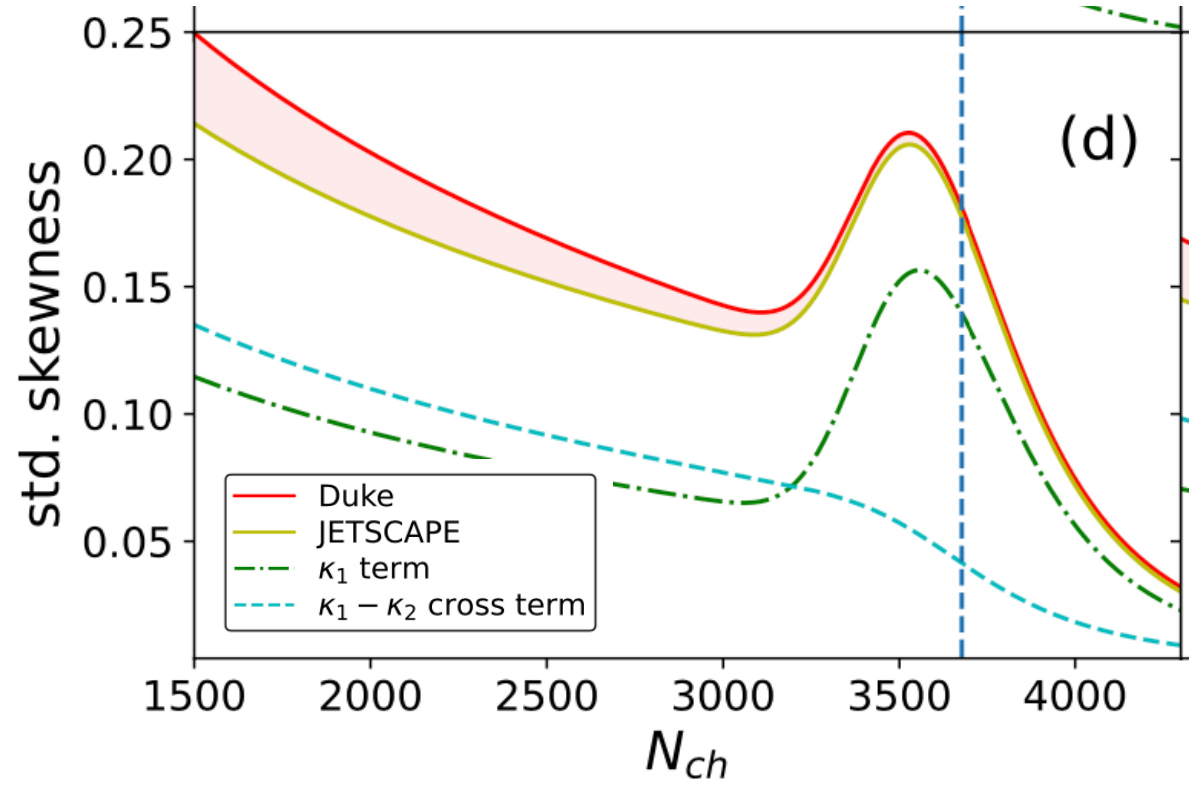

[R. Samanta et al., PRC 108 (2023) 024908]

Skewness of $[p_{\mathrm{T}}]$ in UCC

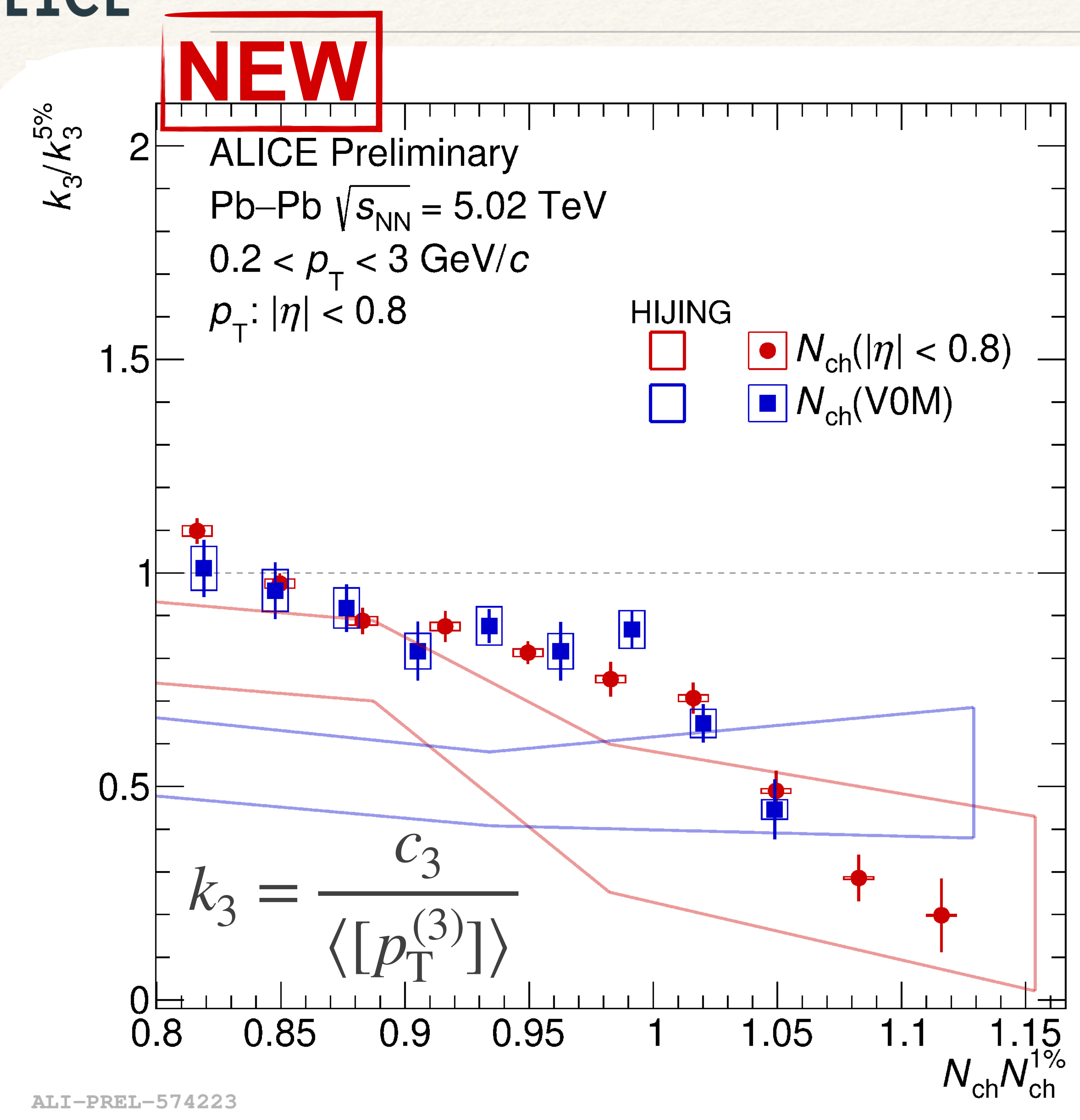

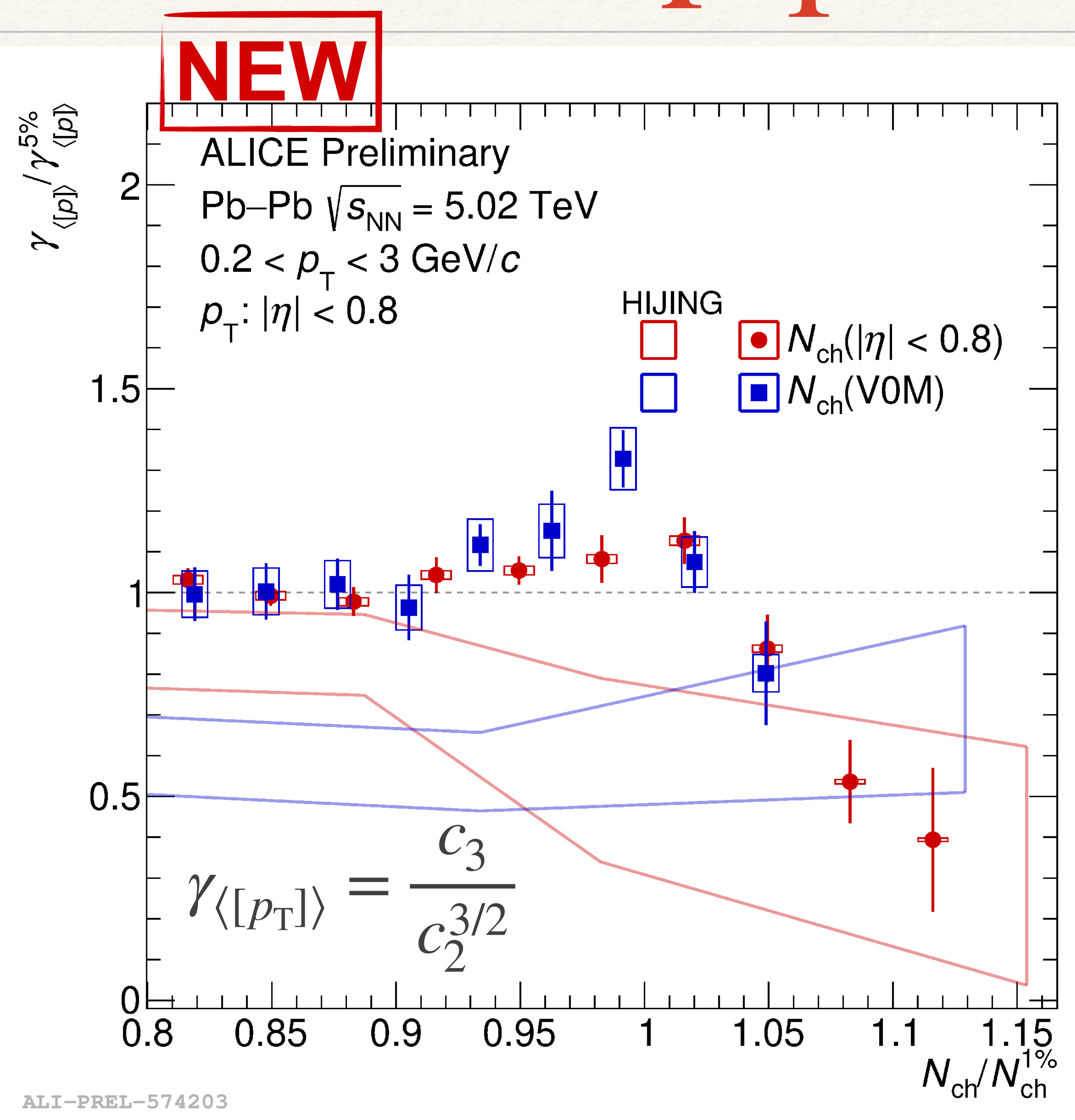

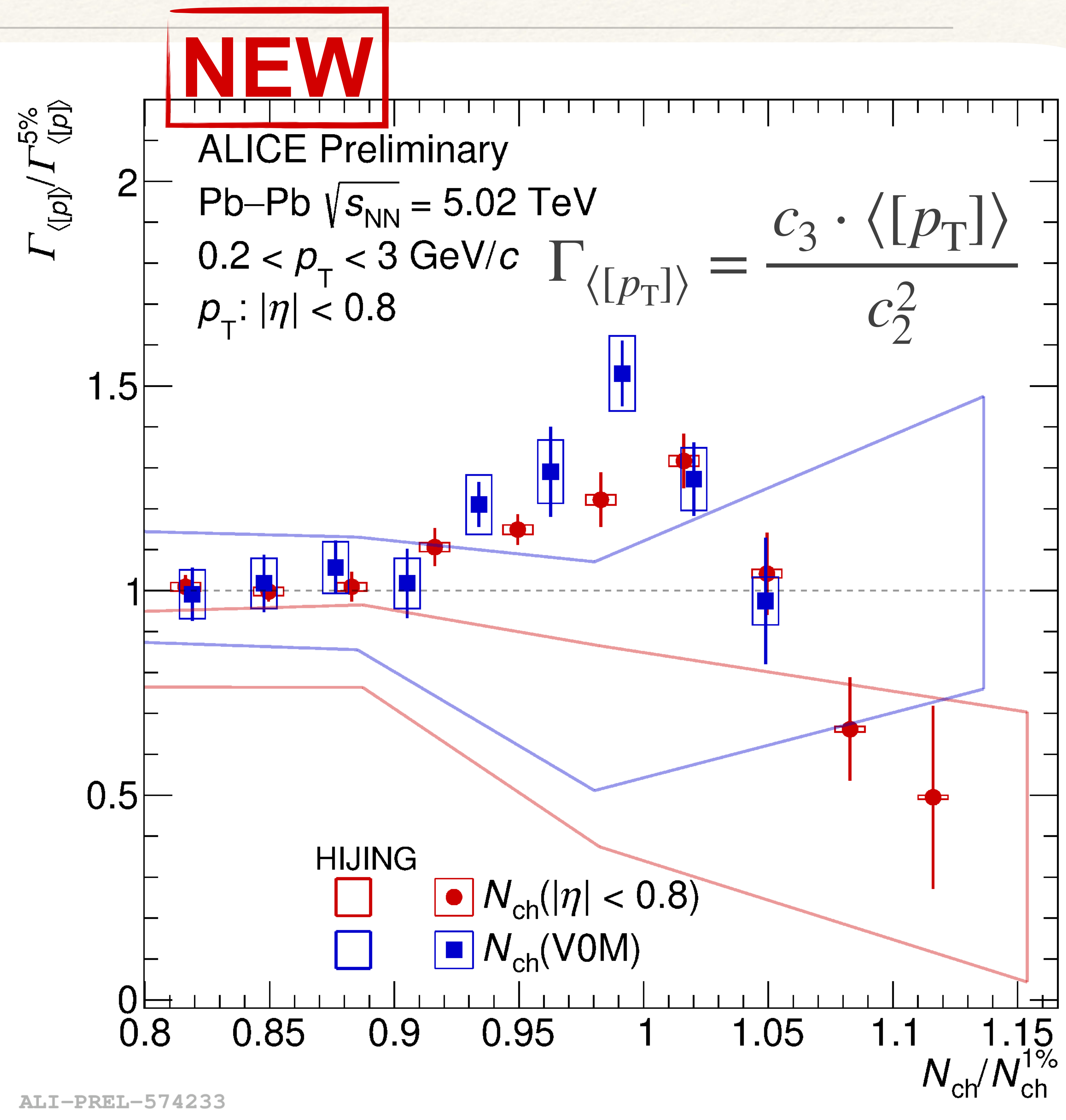

- Skewness behaviour depends on normalisation
- Interplay between skewness and variance in $\gamma_{\langle[p_{\mathrm{T}}]\rangle}$ and $\Gamma_{\langle[p_{\mathrm{T}}]\rangle}$
- Bump driven by geometrical fluctuations

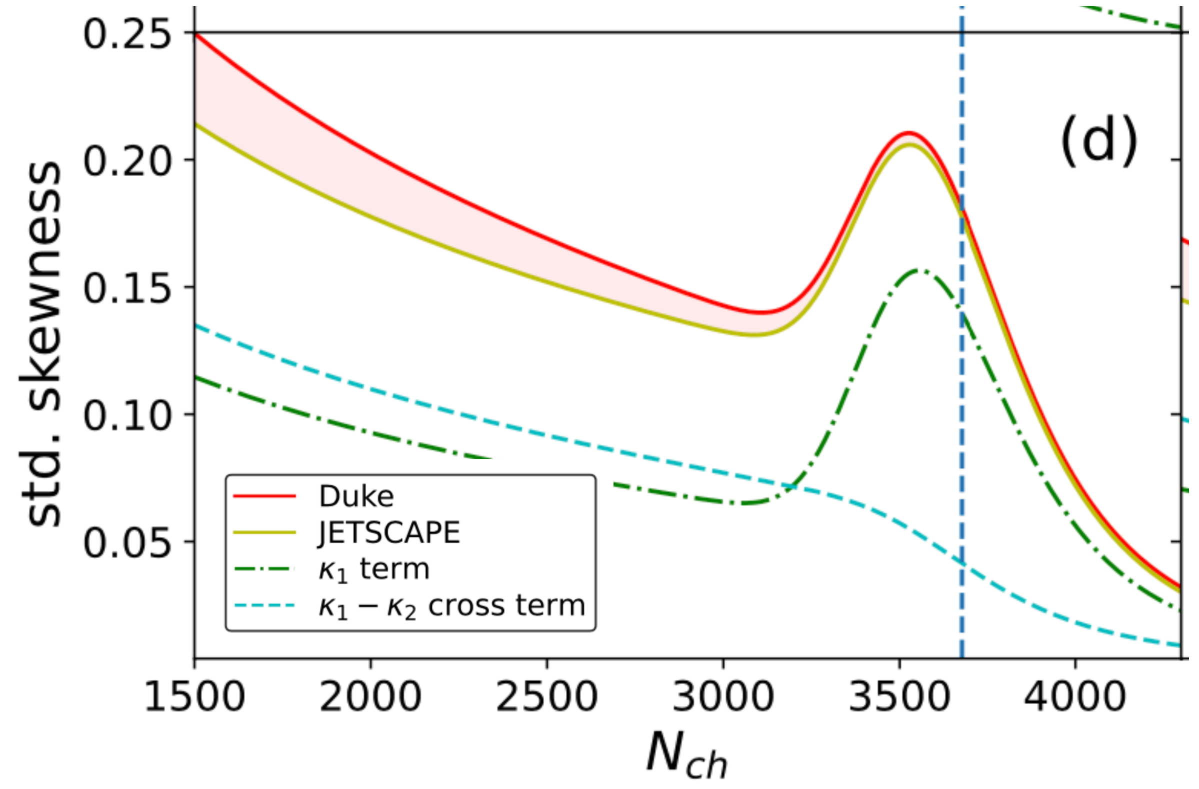

[R. Samanta et al., PRC 108 (2023) 024908]

Skewness of $[p_T]$ in UCC

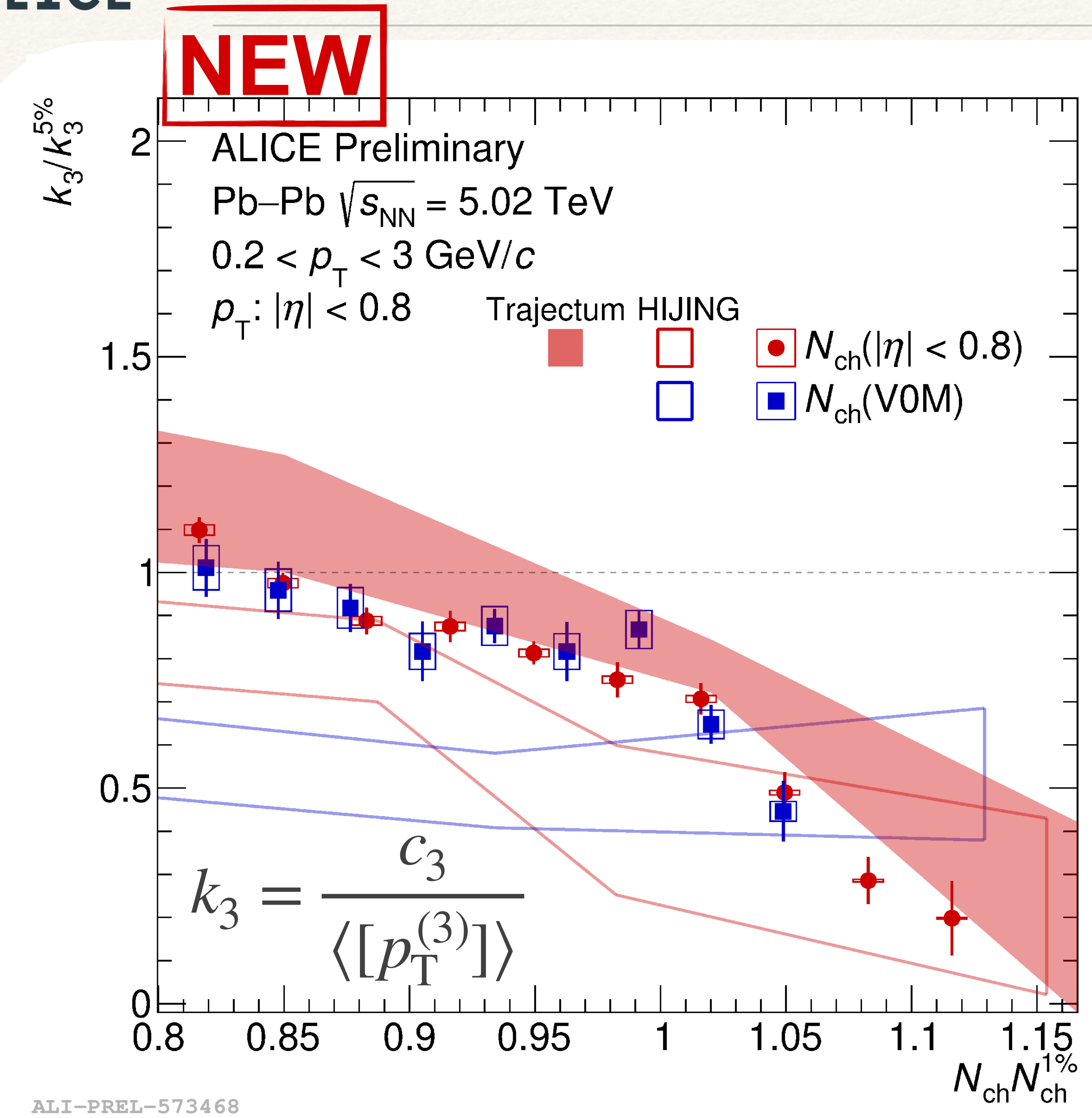

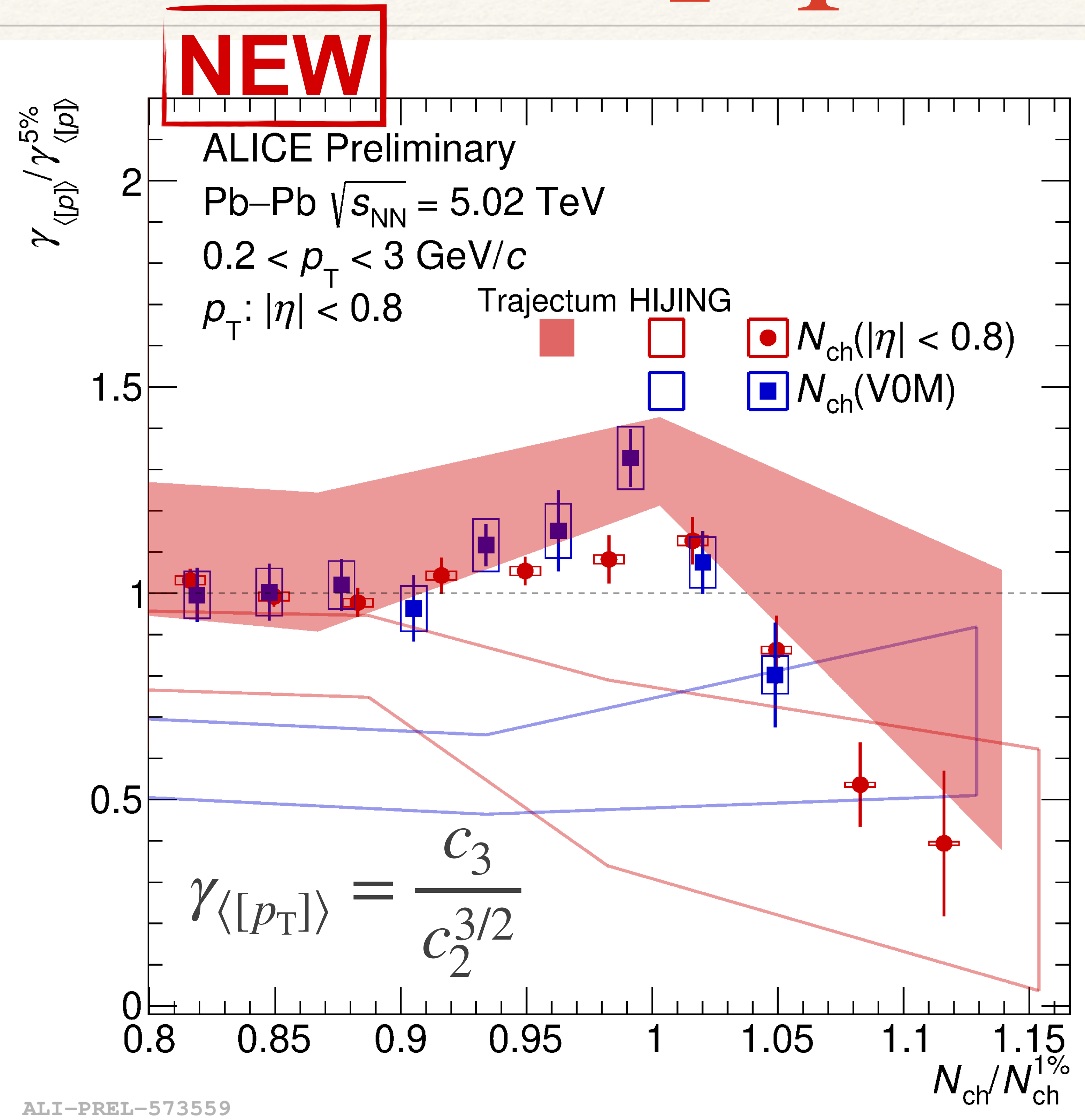

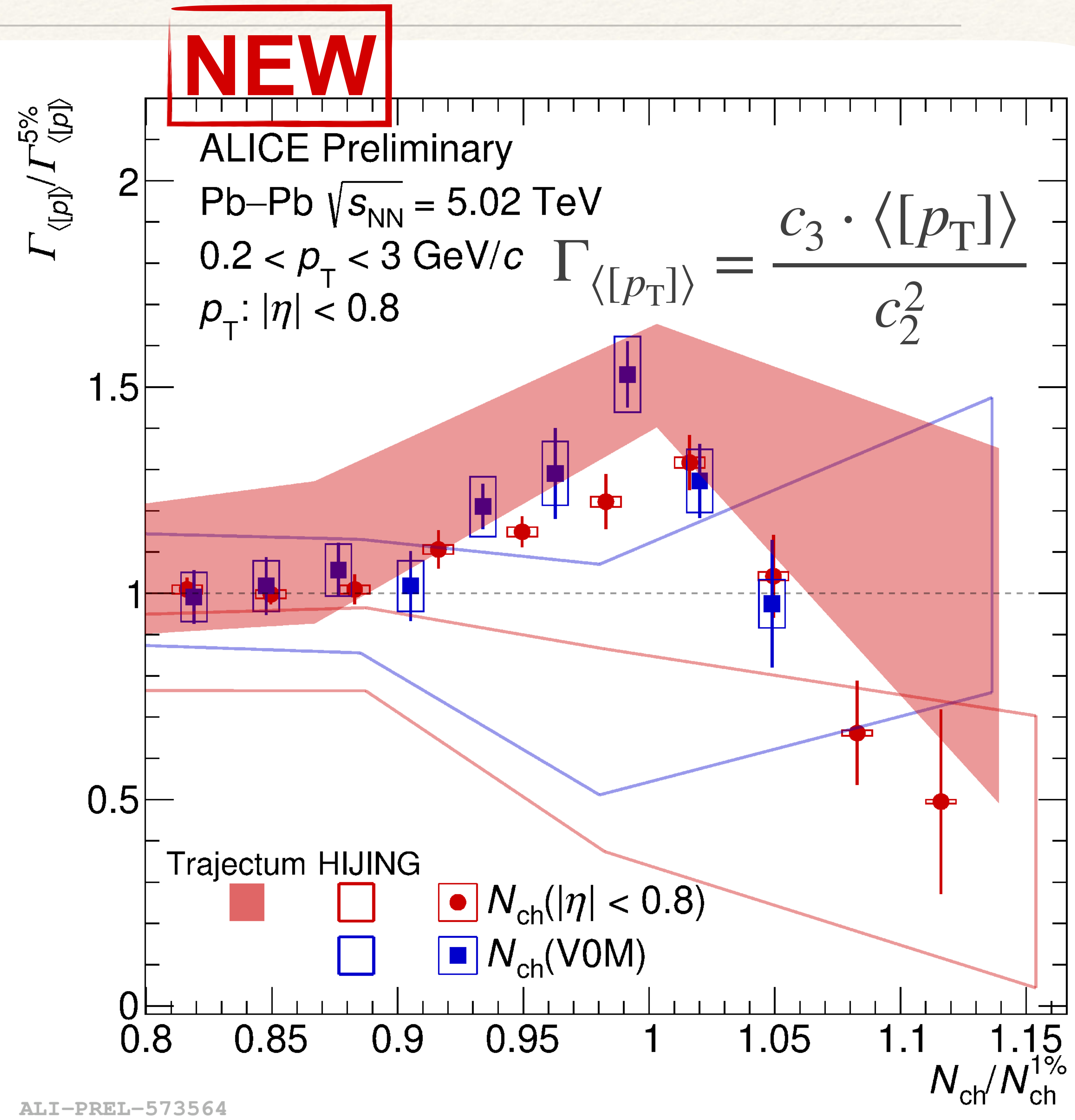

- Variations are features of a thermalised system
- Sensitive to early thermodynamic properties at highest QGP temperatures

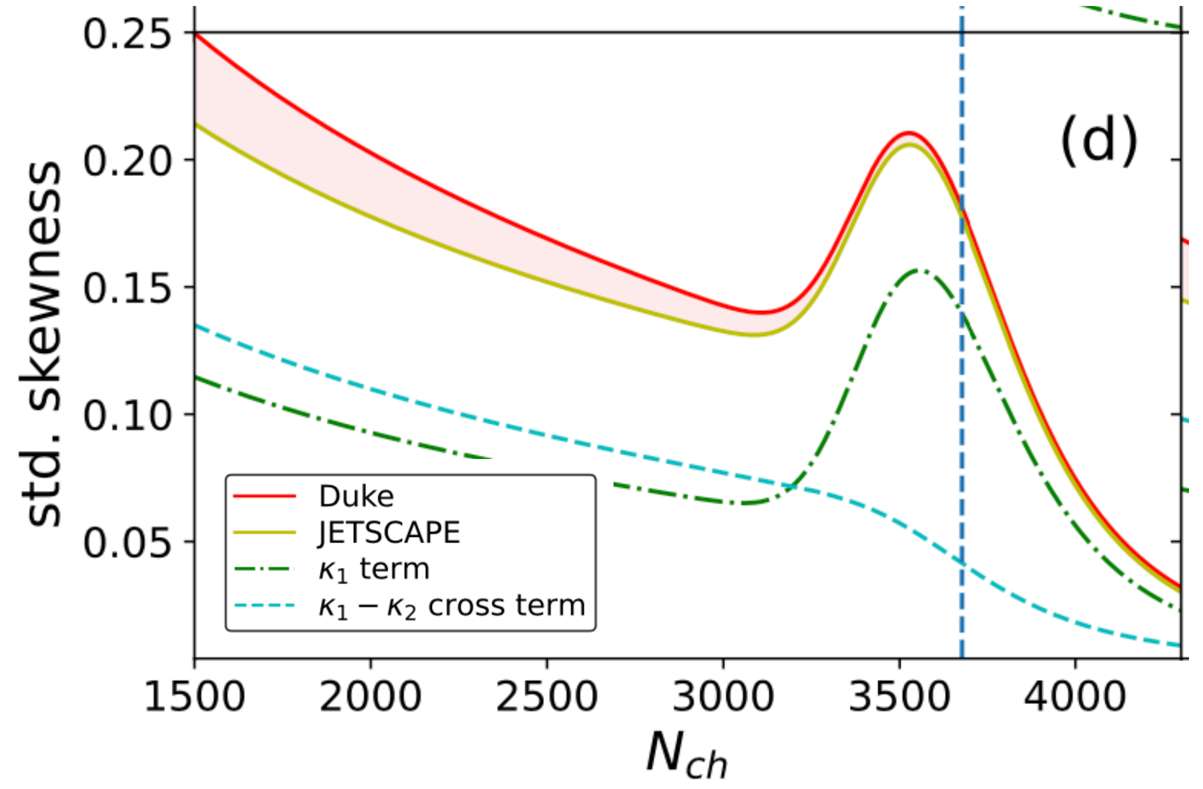

[R. Samanta et al., PRC 108 (2023) 024908]

Kurtosis of $[p_\mathrm{T}]$ in UCC

- Decrease of the kurtosis followed by significant increase
- Effect is lessened when determined as function of forward N_ch

[R. Samanta et al., PRC 108 (2023) 024908]

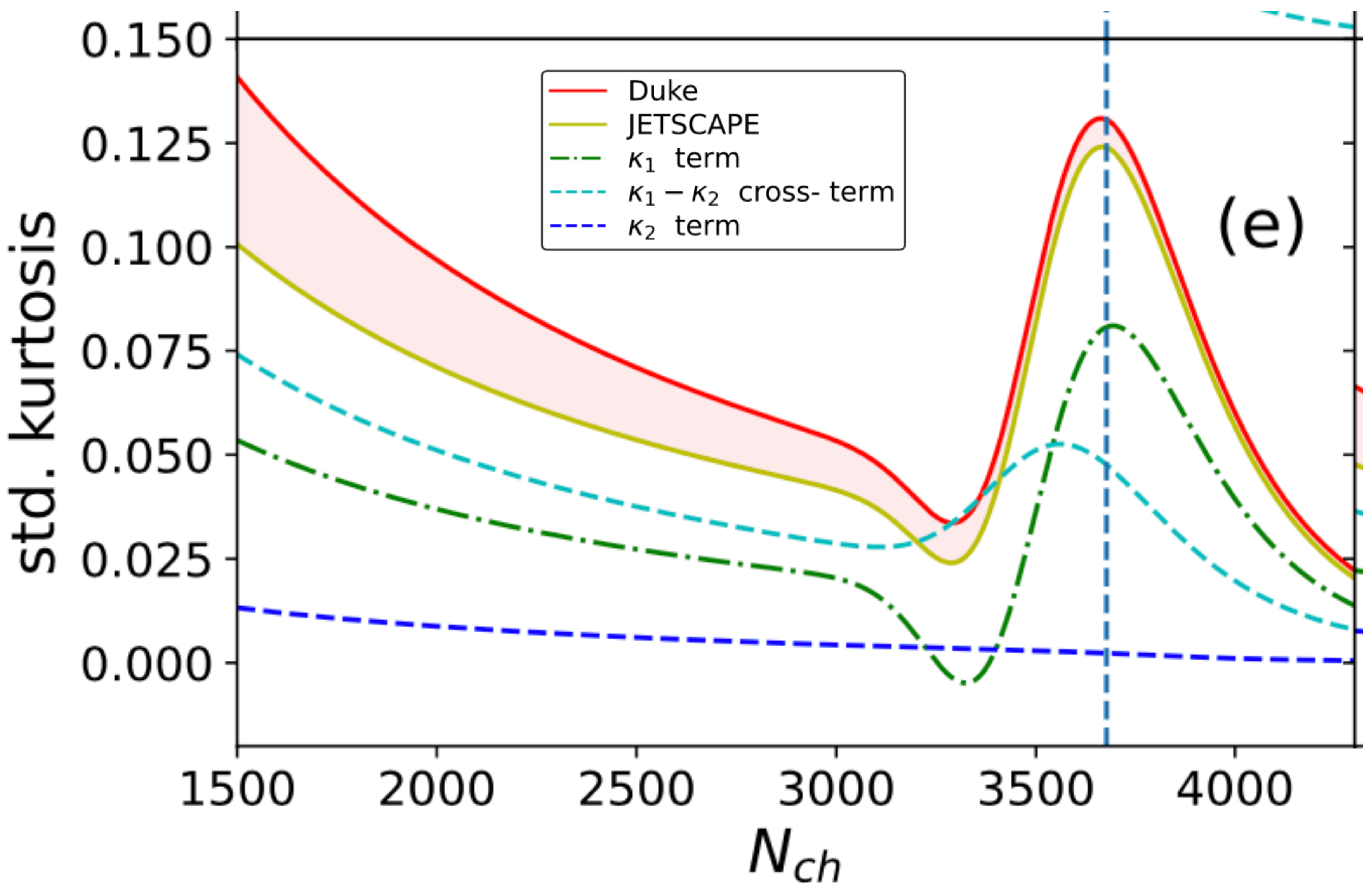

NEW

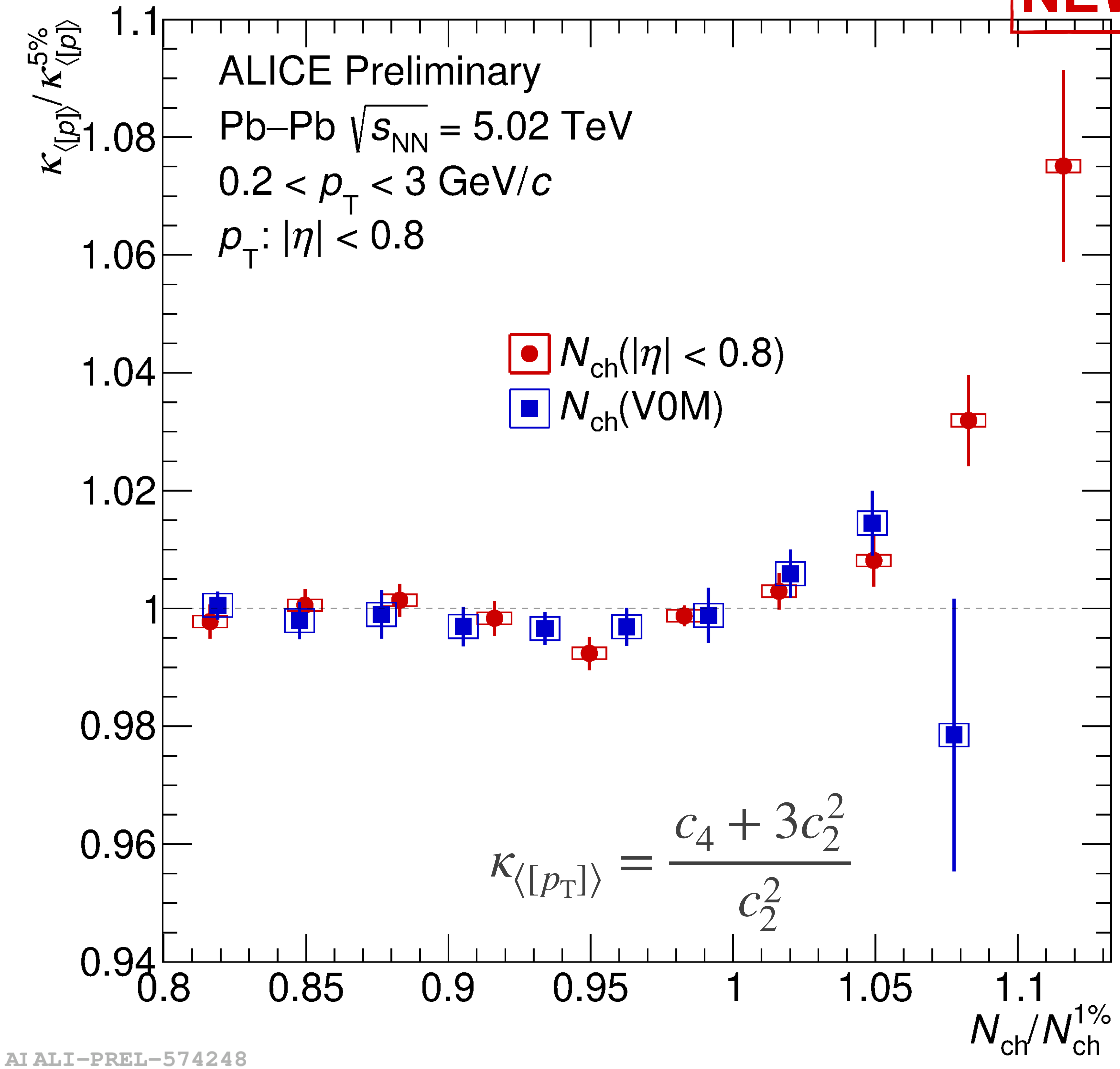

Kurtosis of $[p_T]$ in UCC

NEW

- Decrease of the kurtosis followed by significant increase
- Effect is lessened when determined as function of forward N_{ch}

[R. Samanta et al., PRC 108 (2023) 024908]

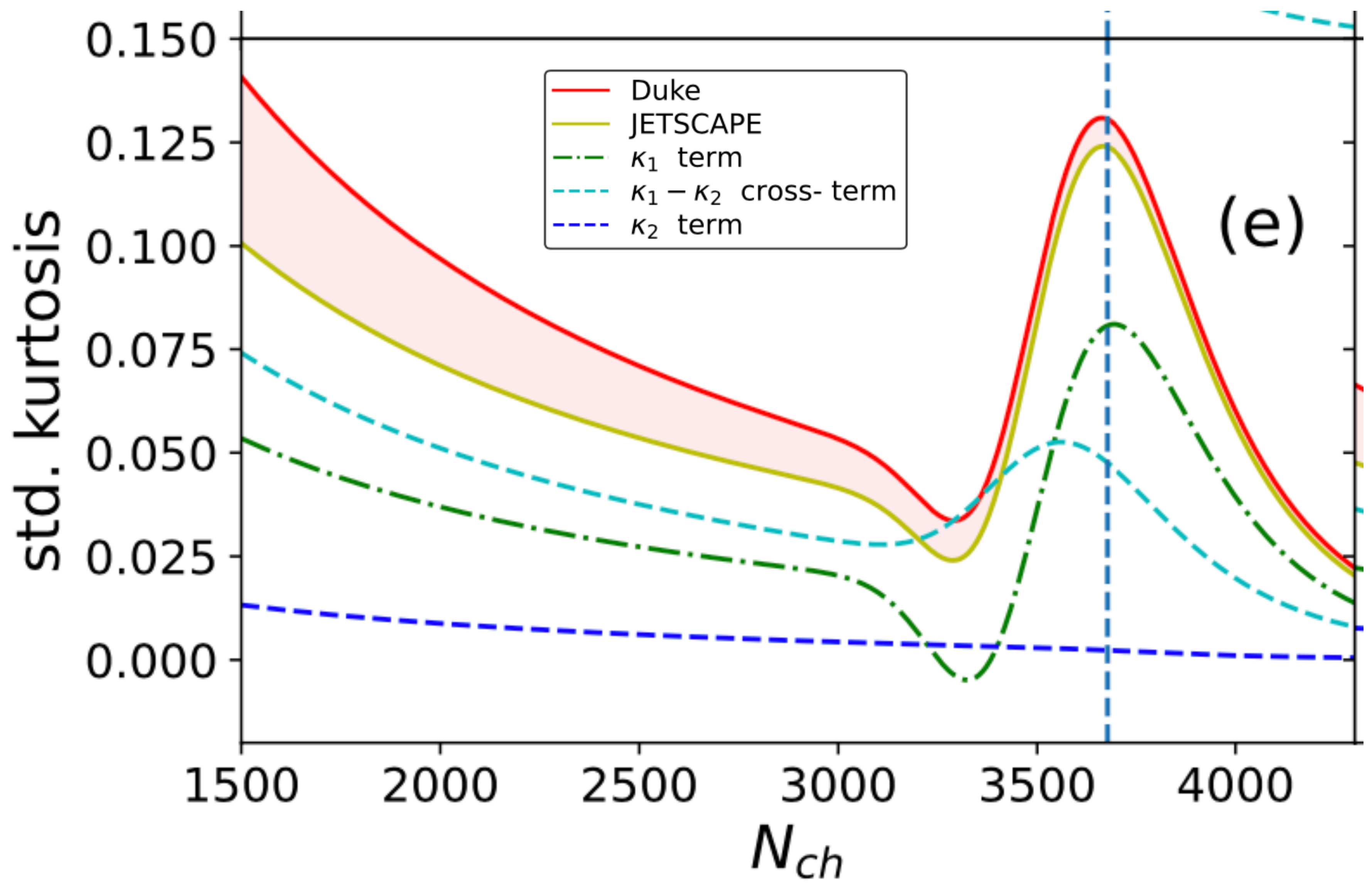

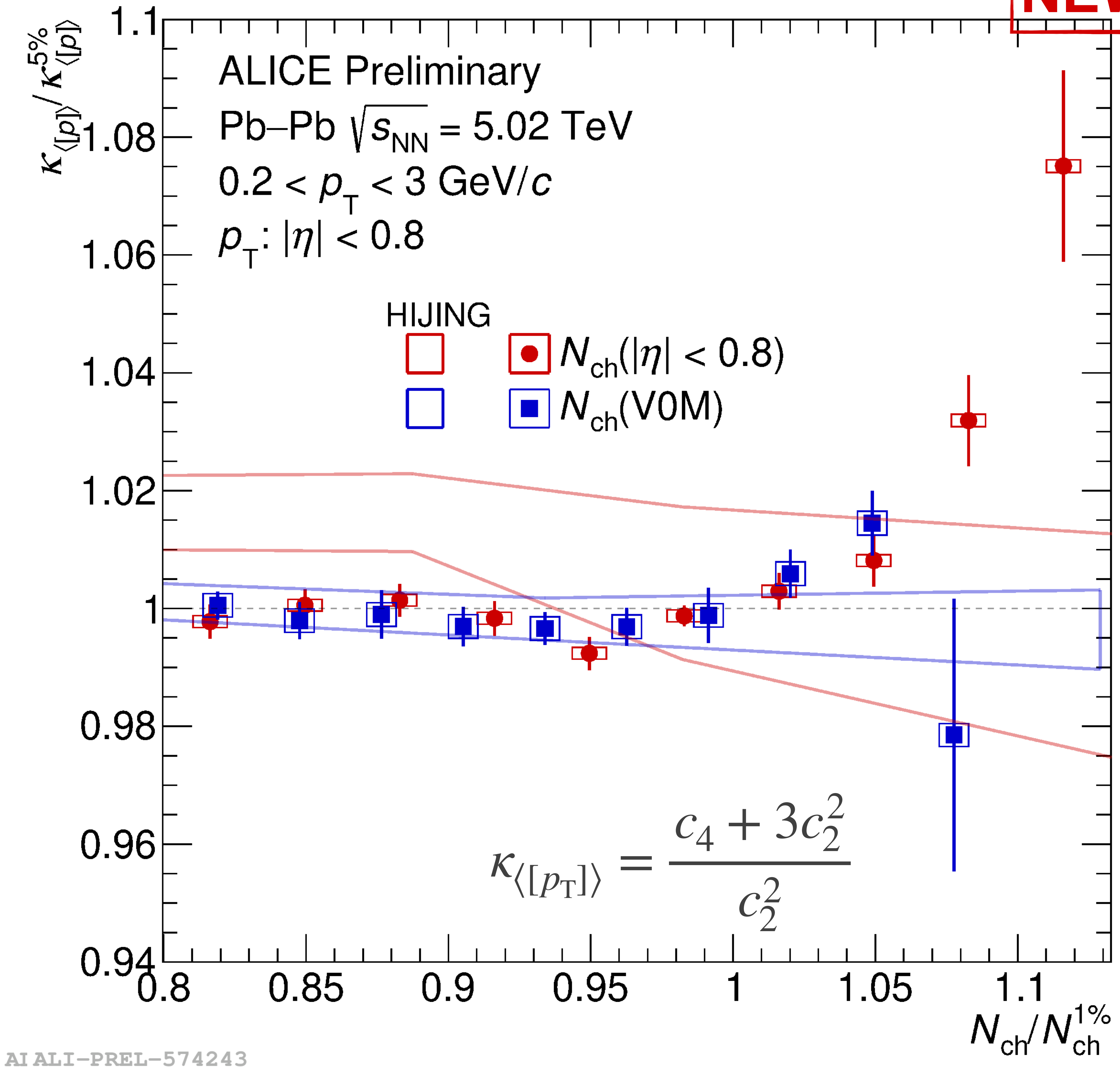

Kurtosis of $[p_\mathrm{T}]$ in UCC

- Decrease of the kurtosis followed by significant increase
- Effect is lessened when determined as function of forward N_ch

[R. Samanta et al., PRC 108 (2023) 024908]

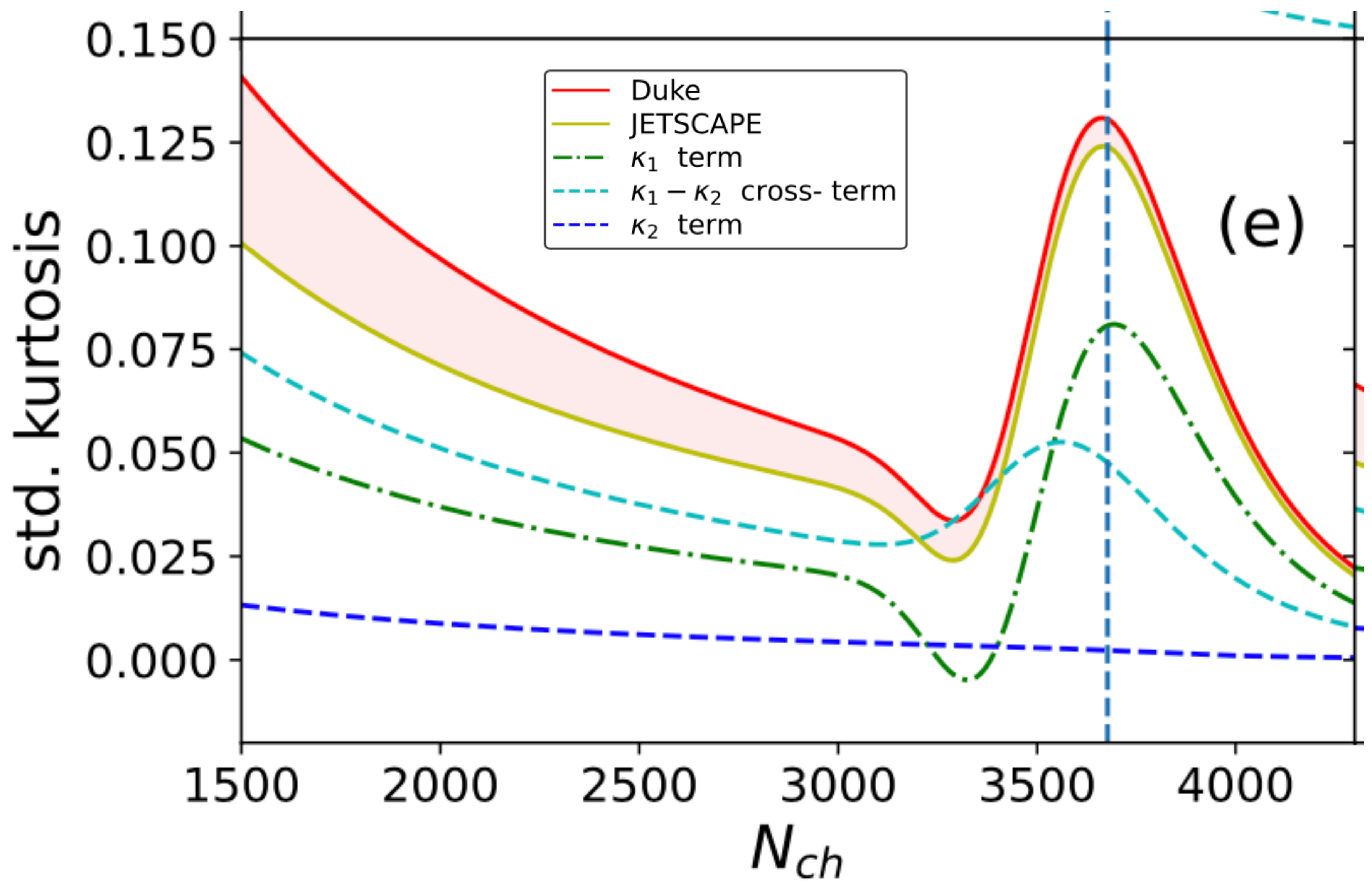

NEW

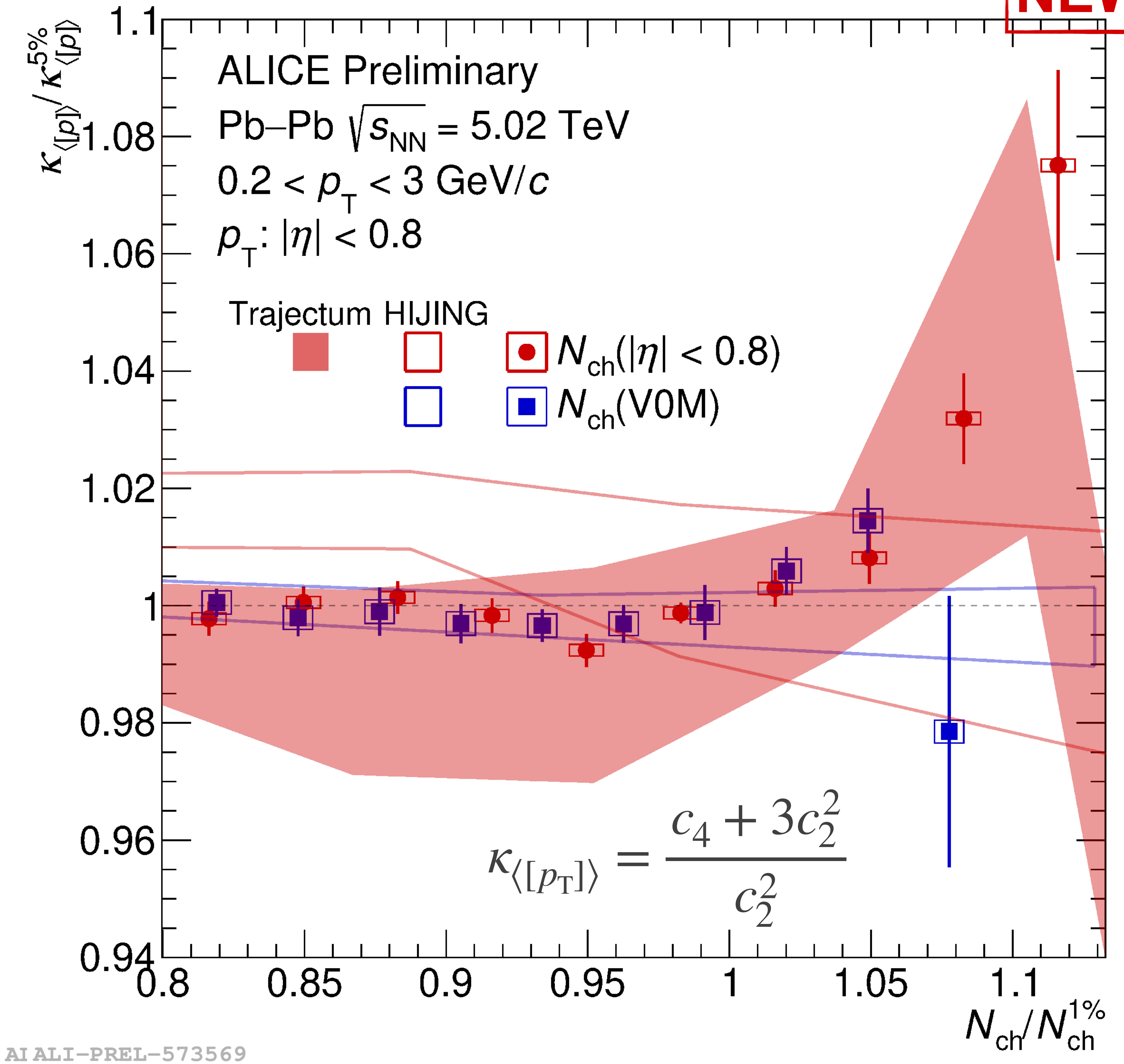

Summary

The correlation between $\langle p_{\mathrm{T}} \rangle$ and N_{ch} in ultra-central collisions - a **feature of a thermalised system** - can be used to extract the speed of sound in the QGP

The extraction is heavily **dependent on the choice of centrality estimator**
A significant difference in forward versus midrapidity centrality determination and from the bias of the centrality estimator

The measurements of the fluctuations of event-by-event mean transverse momentum exhibit **significant changes in ultra-central collisions**
In Gaussian model: driven by the changes in geometrical fluctuations and the remaining intrinsic fluctuations
In hydrodynamic models: Further contributions from the non-gaussian fluctuations of the initial state of the QGP

The data is **well described by a state-of-art hydrodynamic model** from which a consistent speed of sound can be extracted
Further constraints on the hydrodynamic models related to the determination of the speed of sound in QGP

Summary

The correlation between $\langle p_{\mathrm{T}} \rangle$ and N_{ch} in ultra-central collisions - a **feature of a thermalised system** - can be used to extract the speed of sound in the QGP

The extraction is heavily **dependent on the choice of centrality estimator**
A significant difference in forward versus midrapidity centrality determination and from the bias of the centrality estimator

The measurements of the fluctuations of event-by-event mean transverse momentum exhibit **significant changes in ultra-central collisions**
In Gaussian model: driven by the changes in geometrical fluctuations and the remaining intrinsic fluctuations
In hydrodynamic models: Further contributions from the non-gaussian fluctuations of the initial state of the QGP

The data is **well described by a state-of-art hydrodynamic model** from which a consistent speed of sound can be extracted
Further constraints on the hydrodynamic models related to the determination of the speed of sound in QGP

Thank you for your attention!

Backup

Formulas

$[p_{\mathrm{T}}]$ cumulants

$$c_2 = \langle [p_{\mathrm{T}}^{(2)}] \rangle - \langle [p_{\mathrm{T}}] \rangle^2$$

$$c_3 = \langle [p_{\mathrm{T}}^{(3)}] \rangle - 3\langle [p_{\mathrm{T}}^2] \rangle \langle [p_{\mathrm{T}}] \rangle + 2\langle [p_{\mathrm{T}}^3] \rangle$$

$$c_4 = \langle [p_{\mathrm{T}}^{(4)}] \rangle - 4\langle [p_{\mathrm{T}}^{(3)}] \rangle \langle [p_{\mathrm{T}}] \rangle - 3\langle [p_{\mathrm{T}}^{(2)}] \rangle^2 + 12\langle [p_{\mathrm{T}}^{(2)}] \rangle \langle [p_{\mathrm{T}}] \rangle^2 - 6\langle [p_{\mathrm{T}}^{(4)}] \rangle$$

Recursive moments

$$\langle [p_{\mathrm{T}}^{(k)}] \rangle = \frac{N\langle k \rangle_{p_{\mathrm{T}}}}{D\langle k \rangle_{p_{\mathrm{T}}}}$$

$$N\langle m \rangle_{p_{\mathrm{T}}} = \sum_{k=1}^{m} (-1)^{k-1} N\langle m\text{-}k \rangle_{p_{\mathrm{T}}} \frac{(m-1)!}{(m-k)!} \sum_{i}^{M} P_{k,k}$$

$$D\langle m \rangle_{p_{\mathrm{T}}} = \sum_{k=1}^{m} (-1)^{k-1} D\langle m\text{-}k \rangle_{p_{\mathrm{T}}} \frac{(m-1)!}{(m-k)!} \sum_{i}^{M} P_{k,0}$$

$[p_{\mathrm{T}}]$ moments

$$P_{n,k} = \sum_{i}^{M} w_i^n p_{\mathrm{T,i}}^k$$

$$\langle [p_{\mathrm{T}}] \rangle = \frac{P_{1,1}}{P_{1,0}}$$

$$\langle [p_{\mathrm{T}}^{(2)}] \rangle = \frac{P_{1,1}^2 - P_{2,2}}{P_{1,0}^2 - P_{2,0}}$$

$$\langle [p_{\mathrm{T}}^{(3)}] \rangle = \frac{P_{1,1}^3 - 3P_{2,2}P_{1,1} + 2P_{3,3}}{P_{1,0}^3 - 3P_{2,0}P_{1,0} + 2P_{3,0}}$$

$$\langle [p_{\mathrm{T}}^{(4)}] \rangle = \frac{P_{1,1}^4 + 8P_{3,3}P_{1,1} - 6P_{2,2}P_{1,1}^2 + 3P_{2,2}^2 - 6P_{4,4}}{P_{1,0}^4 + 8P_{3,0}P_{1,0} - 6P_{2,0}P_{1,0}^2 + 3P_{2,0}^2 - 6P_{4,0}}$$

Fitting the $\langle p_{\mathrm{T}} \rangle$

Correlation between $\langle p_{\mathrm{T}} \rangle$ and N_{ch} fitted with parametrisation based on PLB 809 (2020) 135749

$$\langle p_{\mathrm{T}} \rangle / \langle p_{\mathrm{T}} \rangle^{\mathrm{ref}} = \left(\frac{N^*_{\mathrm{ch}}}{f(N^*_{\mathrm{ch}}, N^*_{\mathrm{ch,knee}}, \sigma_0)} \right)^{c_s^2}$$ where

$$\boxed{f(N^*_{\mathrm{ch}}, N^*_{\mathrm{ch,knee}}, \sigma_0) = N^*_{\mathrm{ch}} - \sigma_0 \sqrt{\frac{2}{\pi}} \frac{\exp\left(-\left[\frac{N^*_{\mathrm{ch}} - N^*_{\mathrm{ch,knee}}}{\sqrt{2}\sigma_0} \right]^2 \right)}{\mathrm{erfc}\left(\frac{N^*_{\mathrm{ch}} - N^*_{\mathrm{ch,knee}}}{\sqrt{2}\sigma_0} \right)}}$$

and $N^*_{\mathrm{ch}} = \langle dN_{\mathrm{ch}}/d\eta \rangle / \langle dN_{\mathrm{ch}}/d\eta \rangle^{\mathrm{ref}}$

$N^*_{\mathrm{ch,knee}}$ and σ_0 obtained from fit to model proposed in PRC 97, 014905 (2018)

Below the knee ($N^*_{\mathrm{ch}} \ll N^*_{\mathrm{ch,knee}}$):

$$f(N^*_{\mathrm{ch}}, N^*_{\mathrm{ch,knee}}, \sigma_0) \approx N^*_{\mathrm{ch}} \rightarrow \langle p_{\mathrm{T}} \rangle / \langle p_{\mathrm{T}} \rangle^{\mathrm{ref}} \approx 1$$

Above the knee ($N^*_{\mathrm{ch}} \gg N^*_{\mathrm{ch,knee}}$):

$$f(N^*_{\mathrm{ch}}, N^*_{\mathrm{ch,knee}}, \sigma_0) \approx N^*_{\mathrm{ch,knee}} \rightarrow \langle p_{\mathrm{T}} \rangle / \langle p_{\mathrm{T}} \rangle^{\mathrm{ref}} \propto \left(\frac{N^*_{\mathrm{ch}}}{N^*_{\mathrm{ch,knee}}} \right)^{c_s^2}$$